Electronic Supplementary Information

Constrained geometry scandium permethylindenyl complexes for the ring-opening polymerisation of *L*- and *rac*-lactide

Nichabhat Diteepeng, Jean-Charles Buffet, Zoë R. Turner and Dermot O'Hare*

Chemistry Research Laboratory, Department of Chemistry, University of Oxford, 12 Mansfield Road, OX1 3TA Oxford, UK.
E-mail: dermot.ohare@chem.ox.ac.uk

Table of Contents

General experiment details

All air- and moisture-sensitive manipulations were carried out using Schlenk line or glove box techniques under an atmosphere of nitrogen. Protio solvents (pentane and benzene) were dried using an MBraun SPS-800 solvent purification system, and stored over THF was dried and refluxed over Na/benzophenone, and collected by distillation. Deuterated solvent (benzene-d_6) was dried over sodium, distilled at reduced pressure, freeze-thaw degassed and stored over pre-activated 3 Å molecular sieves. Chloroform-*d* was used as received for non-sensitive samples. Solution NMR samples were prepared under a nitrogen atmosphere in a glove box, in 5 mm Wilmad NMR tubes equipped with Young's Teflon valves. ^{1}H, ^{13}C{^{1}H} and ^{11}B NMR spectra were recorded on Bruker Advance III 400 spectrometer at 298 K unless stated otherwise. ^{1}H and ^{13}C{^{1}H} spectra were referenced internally to residual protio-solvent (^{1}H) or solvent (^{13}C) resonances, and are reported relative to tetramethylsilane (δ = 0 ppm). Chemical shifts are quoted in δ (ppm) and coupling constants (*J*) in Hz. Assignments were confirmed using two dimensional ^{1}H-^{1}H (COSY), ^{13}C-^{1}H (HSQC and HMBC). ^{1}H{^{1}H} (homonuclear decoupled) NMR experiments were performed with a Bruker Advance III 400 spectrometers at ambient temperature. The tacticity of PLA was analysed by ^{1}H{^{1}H} NMR spectroscopy. P_r values were calculated from integration obtained from ^{1}H{^{1}H} NMR spectra. Alternatively, peak deconvolution, using the Mestrenova software package, was used to improve accuracy in the determination.[1] The probability of a particular tetrad can be calculated using Bernoullian statistics.[2] IR spectra were recorded on a Thermo Scientific Nicolet iS5 FTIR spectrometer. Samples were prepared in a glove box as Nujol mulls between NaCl plates in a NaCl cell. Elemental analysis was carried out by Mr. Stephen Boyer (London Metropolitan University). MALDI-ToF MS analysis was performed by Dr Victor Mikhailov (University of Oxford) using a Bruker MALDI autoflex TOF mass spectrometer. The polymer samples were dissolved in THF at a concentration of 1.0 mg mL^{-1}. The cationising agent used was potassium trifluoroacetate (Fluka, >99%) dissolved in THF at a concentration of 5 mg mL^{-1}. The matrix used was *trans*-2-[3-(4-*tert*-butylphenyl)-2-methy-2-propenylidene]malononitrile (DCTB) (Fluka) dissolved in THF at a concentration of 40.0 mg mL^{-1}. Solutions of matrix, cationising agent and polymer were mixed in a volume ratio of 4:1:4, respectively. The mixed solution was hand-spotted on a stainless steel MALDI plate and left to dry. The spectra were recorded in positive reflectron mode. External instrument calibration was performed using a mixture of standard peptides. Data was analysed with MassLynx.

Polymer molecular weights (M_n, M_w and M_w/M_n) were determined by GPC using a Polymer Laboratories PL-GPC50 Plus instrument equipped with a Polymer Laboratories PLgel Mixed-D column (300 mm length, 7.5 mm diameter) and a refractive index (RI) detector. Chloroform (Fisher, HPLC grade) was used as an eluent at 30 °C with a flow rate of 1.0 mL min^{-1}. Samples were dissolved in chloroform (Fisher, HPLC grade) at a concentration of 3.3 mg mL^{-1} and filtered before injection. Linear polystyrenes (Polymer Laboratories) were used as primary calibration standards and correction factor of 0.58 was applied to calculate the experimental molecular weights.[3]

Representative NMR spectra of ^{Me_2}SB(^{tBu}N,I*)Li$_2$(THF)$_{0.25}$ and complexes 1–4.

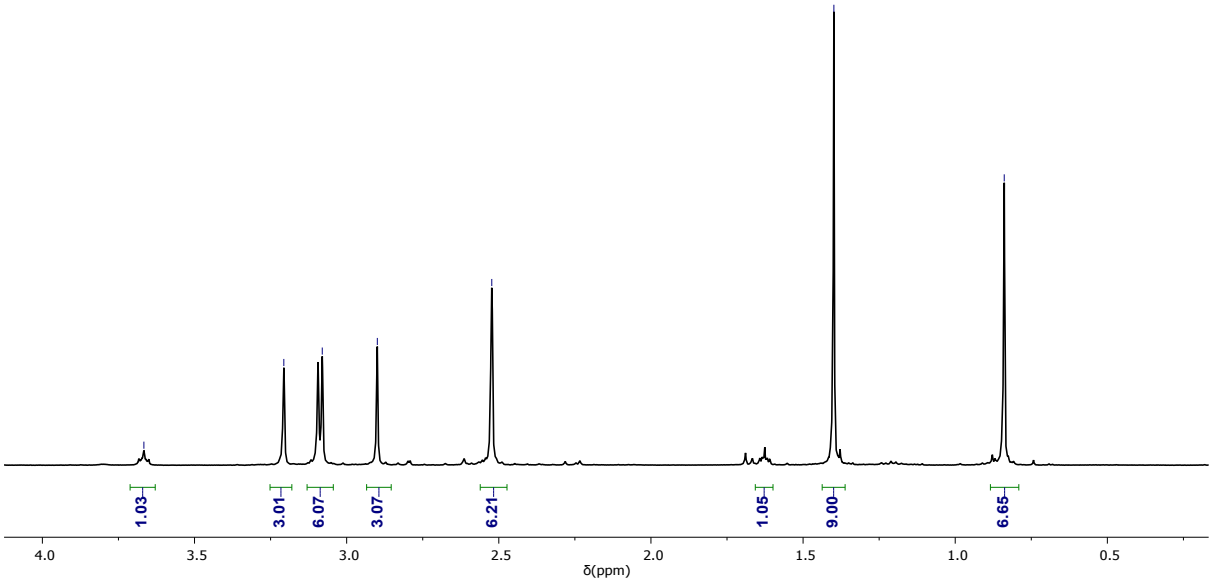

Fig. S1 ^{1}H NMR spectrum (C_5D_5N, 400.2 MHz, 298 K) of ^{Me_2}SB(^{tBu}N,I*)Li$_2$(THF)$_{0.25}$. Solvent resonances at 8.73, 7.59 and 7.22 ppm excluded for clarity.

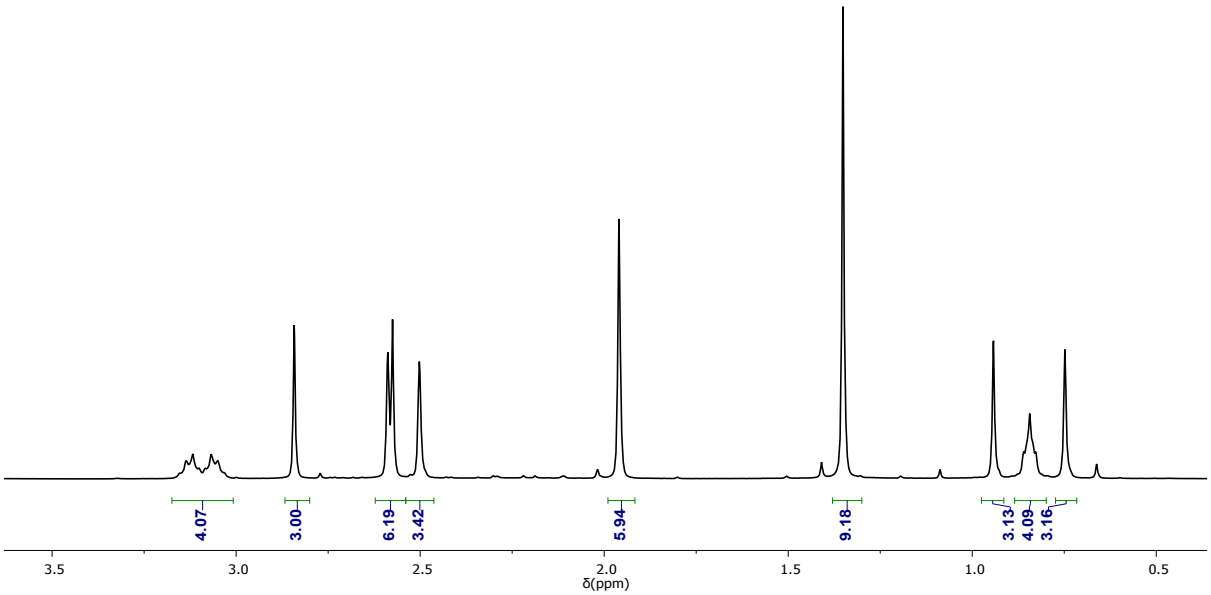

Fig. S2 ^{1}H NMR spectrum (C_6D_6, 400.2 MHz, 298 K) of ^{Me_2}SB($^{t\text{Bu}}$N,I*)Sc(Cl)(THF) (**1**). Solvent resonance at 7.16 ppm excluded for clarity.

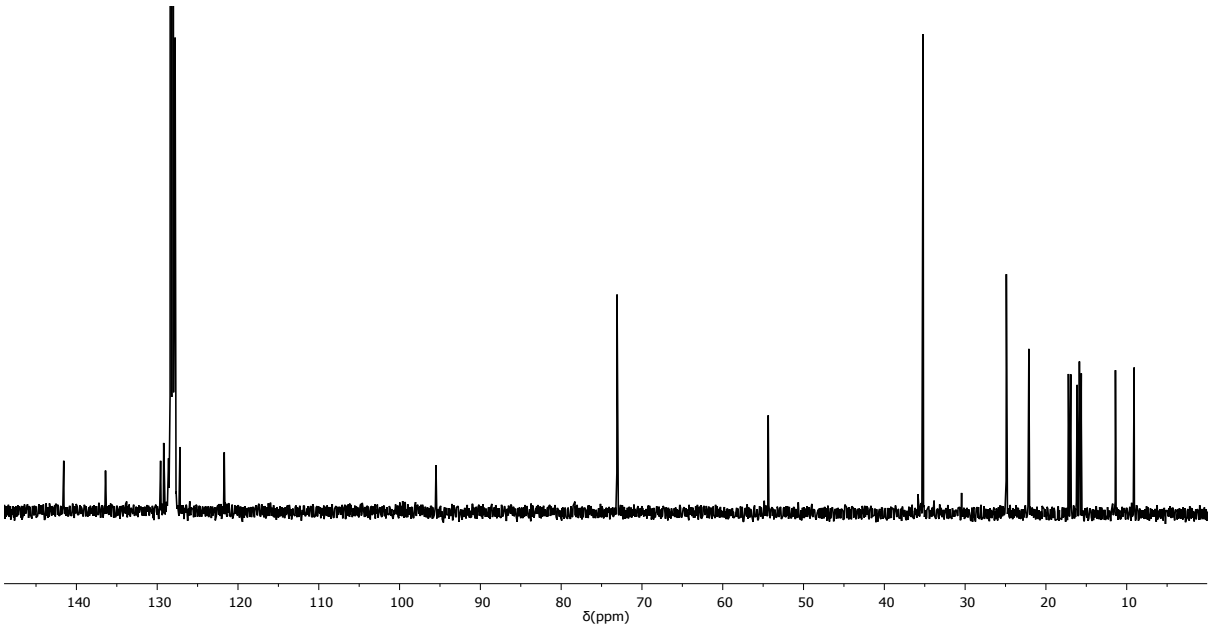

Fig. S3 ^{13}C{^{1}H} NMR spectrum (C_6D_6, 125.8 MHz, 298 K) of ^{Me_2}SB($^{t\text{Bu}}$N,I*)Sc(Cl)(THF) (**1**).

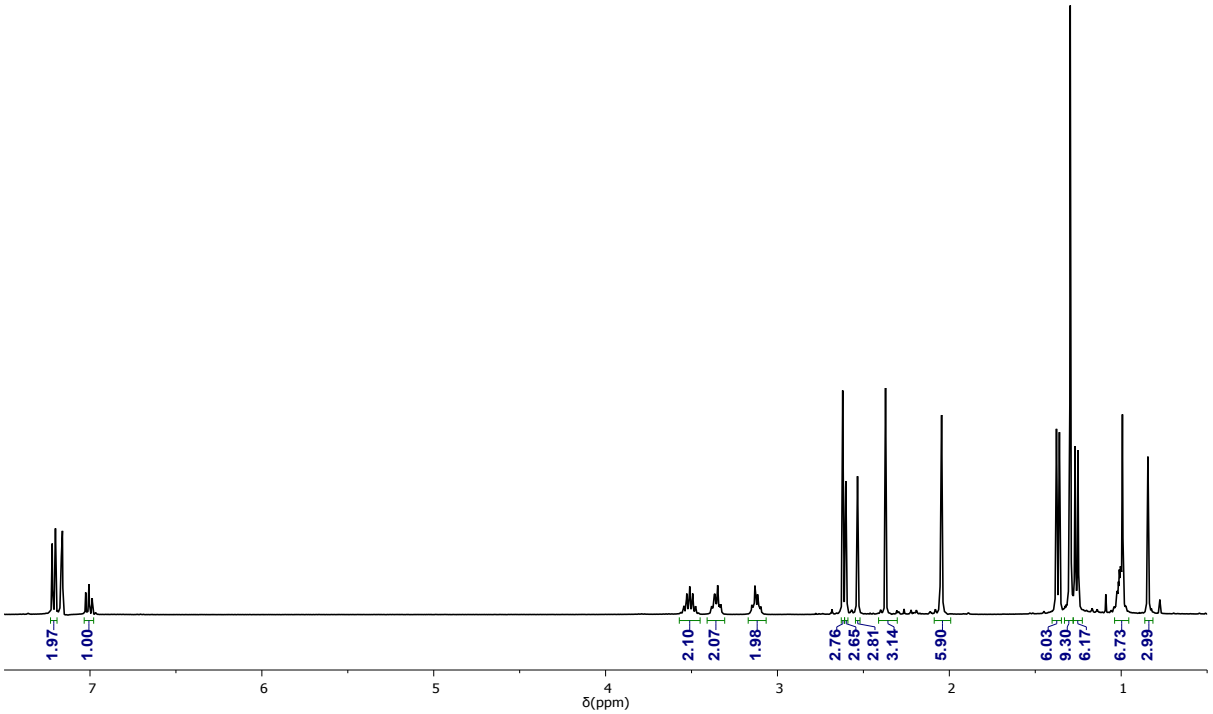

Fig. S4 ^{1}H NMR spectrum (C_6D_6, 400.2 MHz, 298 K) of ^{Me_2}SB(^{tBu}N,I*)Sc(O-2,6-^{i}Pr-C_6H_3)(THF) (**2**).

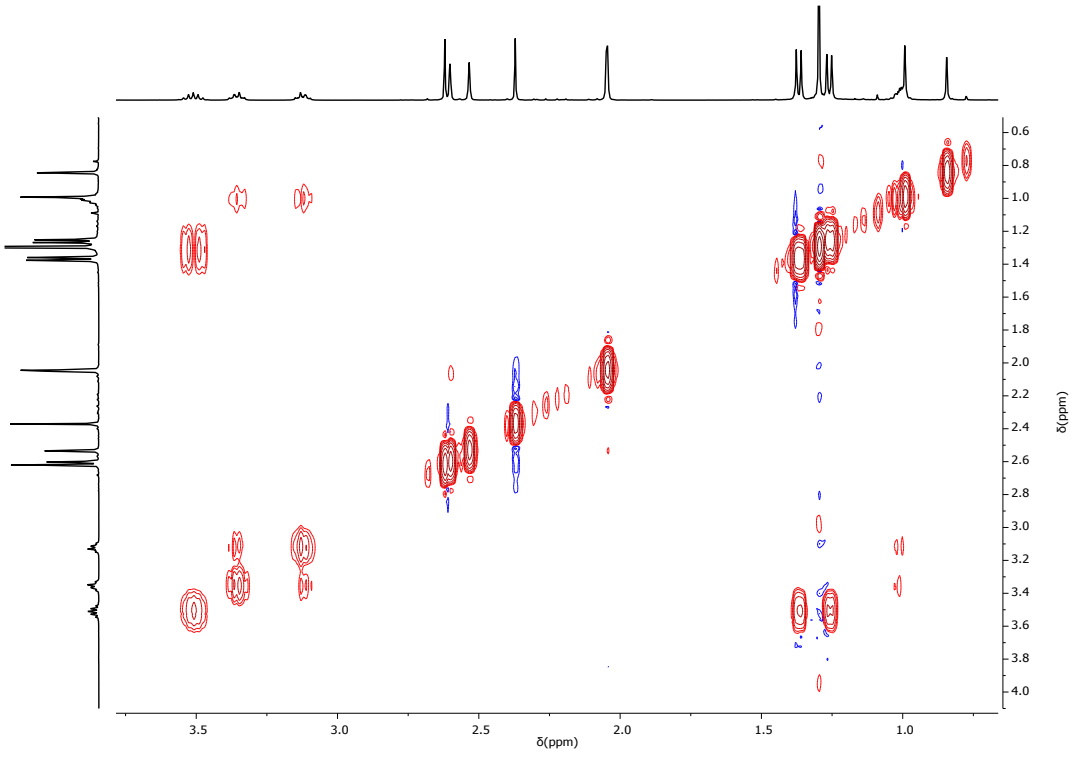

Fig. S5 COSY NMR spectrum (C_6D_6, 400.2 MHz, 298 K) of ^{Me_2}SB(^{tBu}N,I*)Sc(O-2,6-^{i}Pr-C_6H_3)(THF) (**2**).

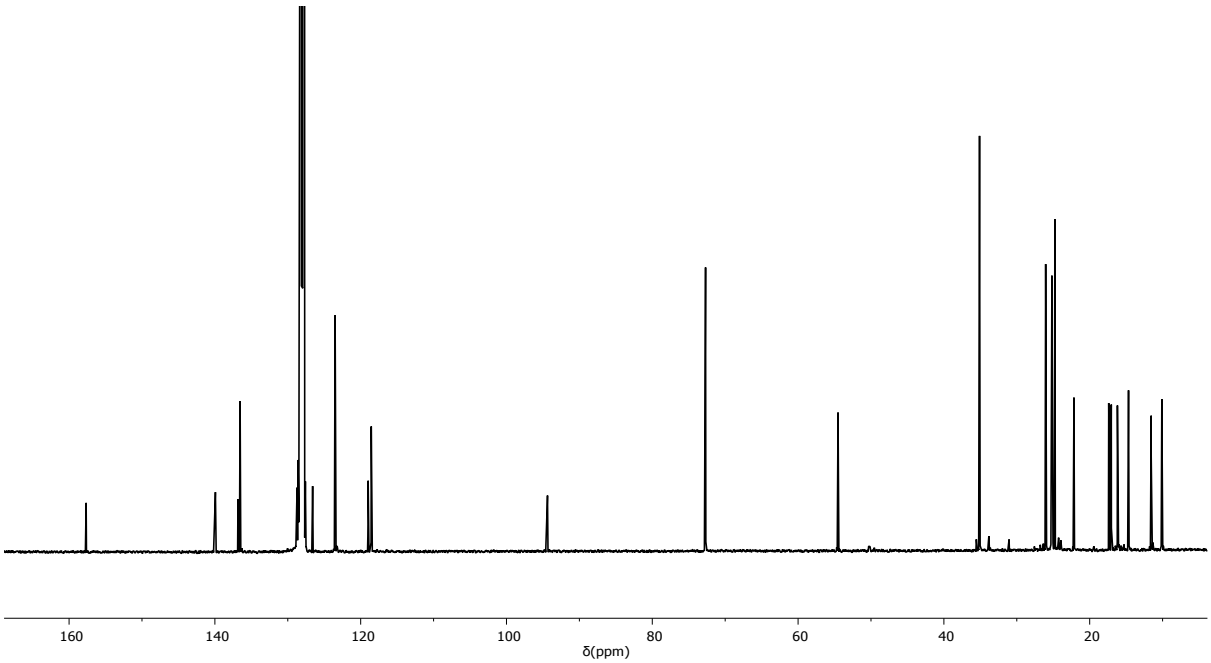

Fig. S6 $^{13}C\{^{1}H\}$ NMR spectrum (C_6D_6, 125.8 MHz, 298 K) of $^{Me_2}SB(^{tBu}N,I^*)Sc(O\text{-}2,6\text{-}^{i}Pr\text{-}C_6H_3)(THF)$ (**2**).

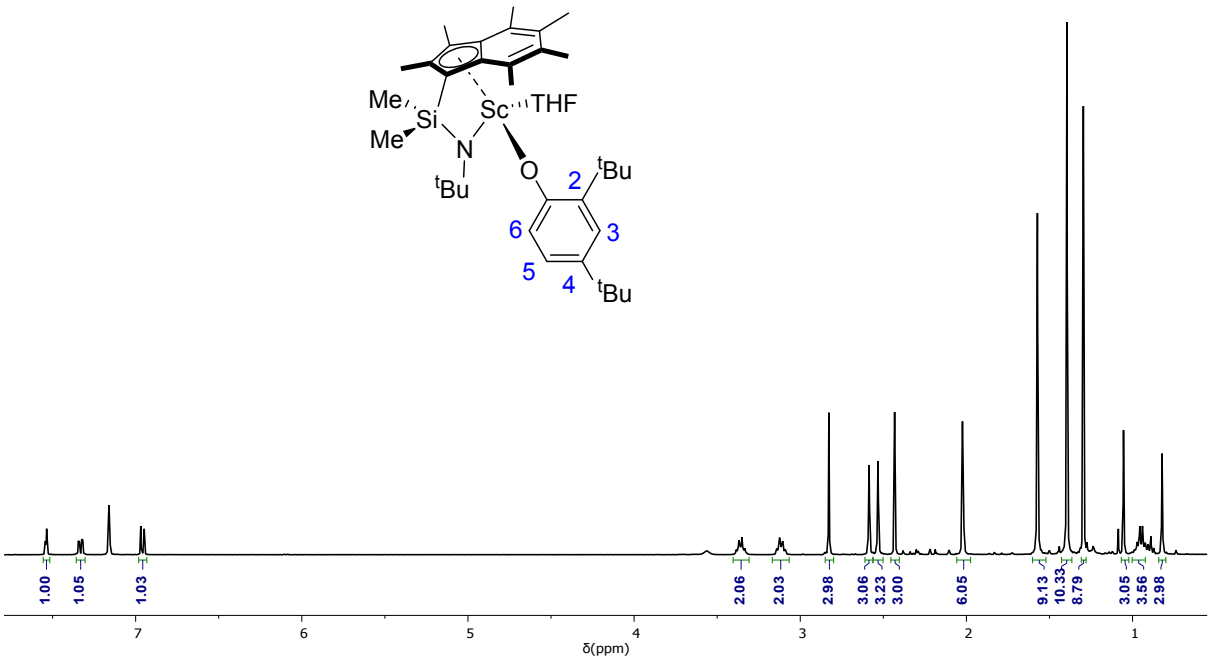

Fig. S7 ^{1}H NMR spectrum (C_6D_6, 400.2 MHz, 298 K) of ^{Me_2}SB($^{t\text{Bu}}$N,I*)Sc(O-2,4-^{t}Bu-C_6H_3)(THF) (**3**).

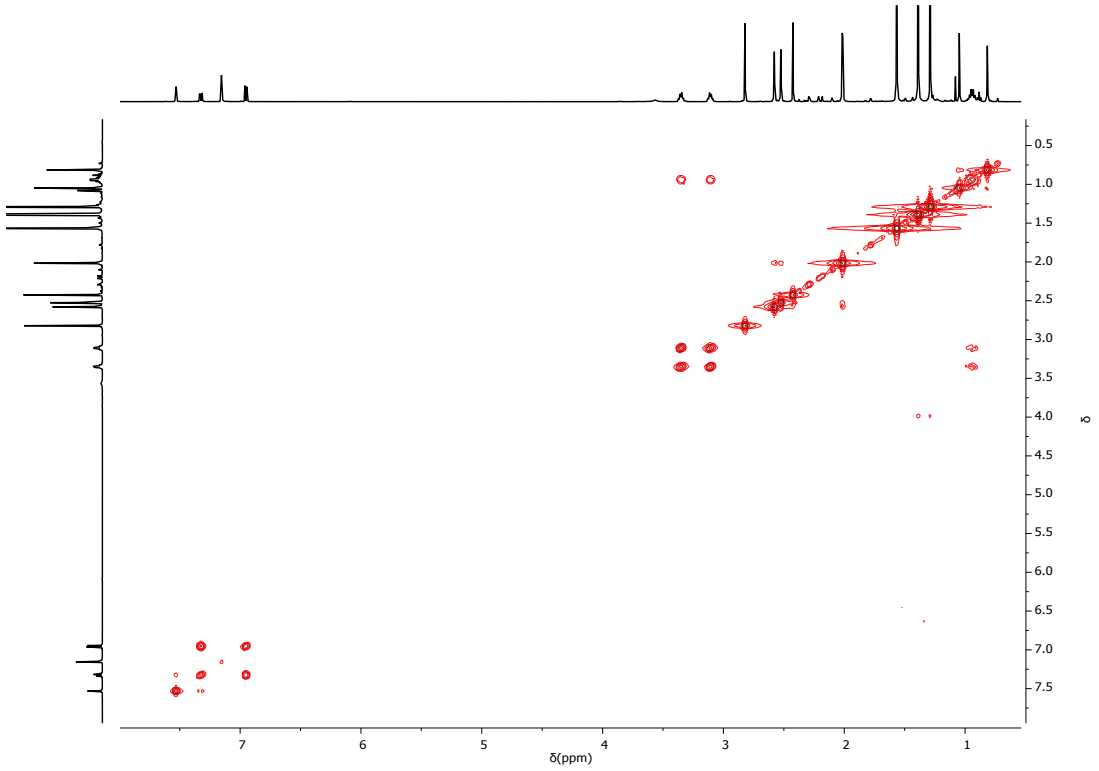

Fig. S8 COSY NMR spectrum (C_6D_6, 400.2 MHz, 298 K) of ^{Me_2}SB($^{t\text{Bu}}$N,I*)Sc(O-2,4-^{t}Bu-C_6H_3)(THF) (**3**).

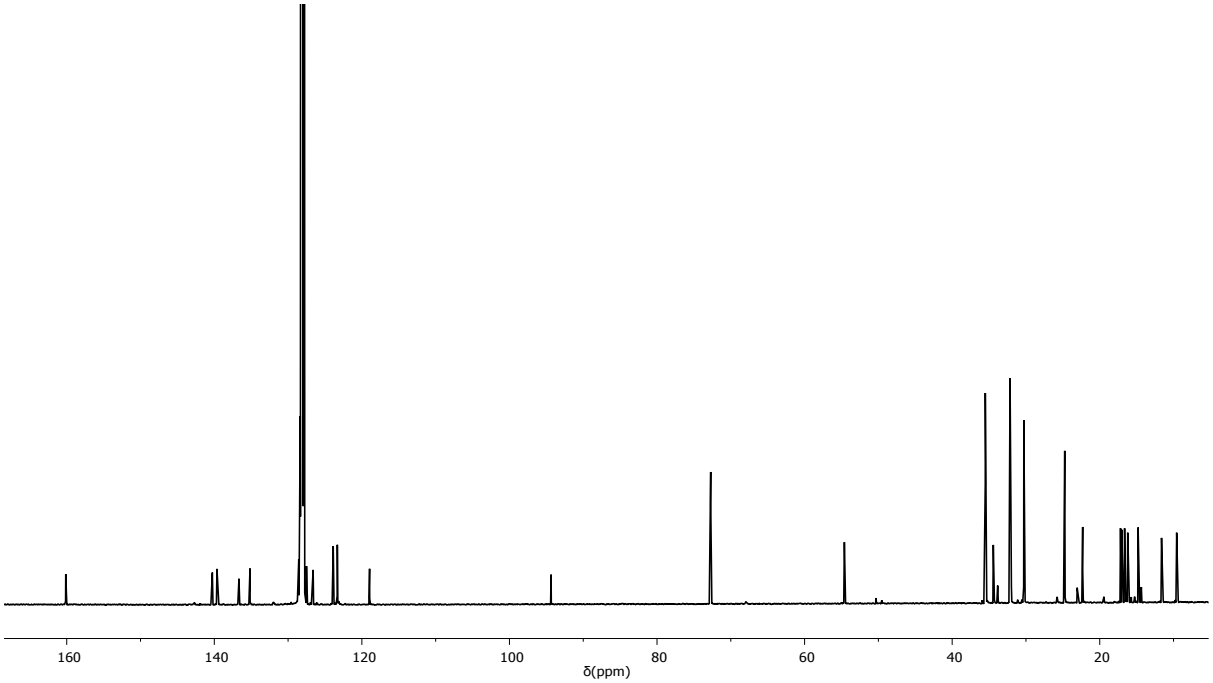

Fig. S9 $^{13}C\{^{1}H\}$ NMR spectrum (C_6D_6, 125.8 MHz, 298 K) of $^{Me}{}_2SB(^{tBu}N,I^*)Sc(O\text{-}2,4\text{-}^{t}Bu\text{-}C_6H_3)(THF)$ (**3**).

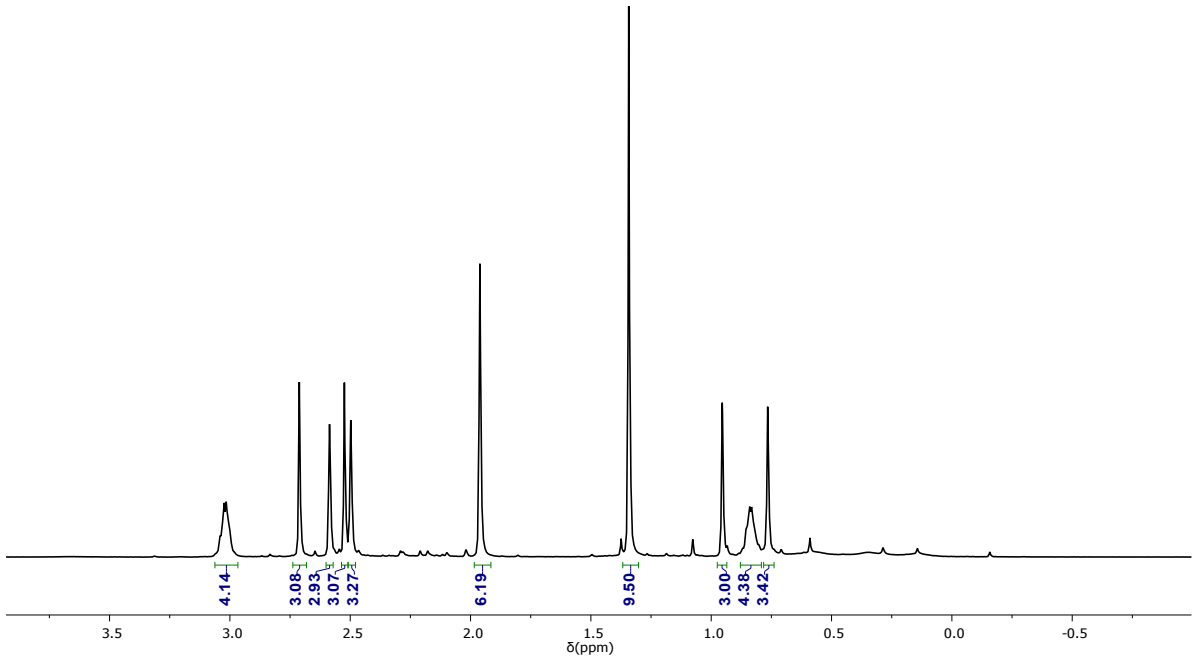

Fig. S10A ^{1}H NMR spectrum (C_6D_6, 400.2 MHz, 298 K) of $^{Me}_2$SB($^{t\text{Bu}}$N,I*)Sc(BH_4)(THF) (**4**). Solvent resonance at 7.16 ppm excluded for clarity.

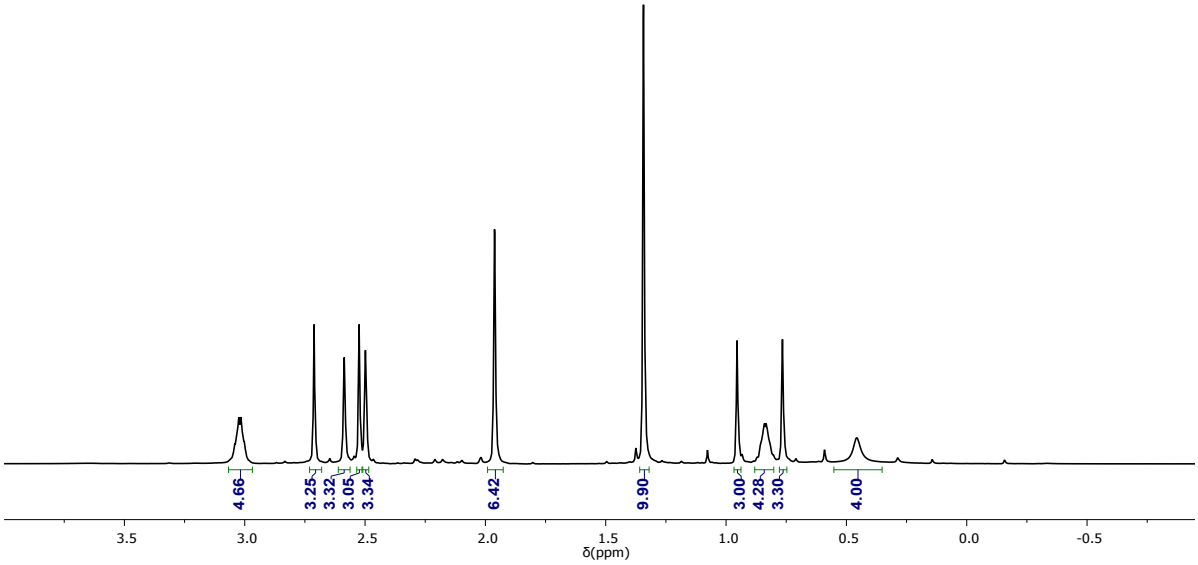

Fig. S10B ^{1}H{^{11}B} NMR spectrum (C_6D_6, 400.2 MHz, 298 K) of $^{Me}_2$SB($^{t\text{Bu}}$N,I*)Sc(BH_4)(THF) (**4**). Solvent resonance at 7.16 ppm excluded for clarity.

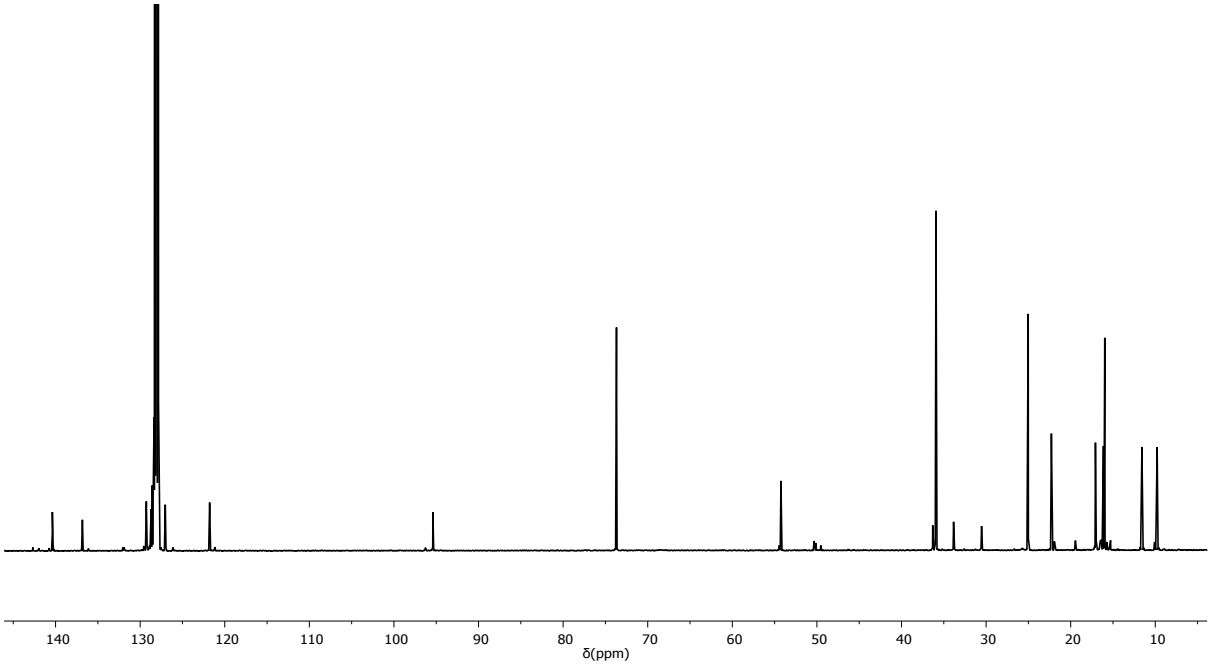

Fig. S11 $^{13}C\{^{1}H\}$ NMR spectrum (C_6D_6, 125.8 MHz, 298 K) of $^{Me_2}SB(^{tBu}N,I^*)Sc(BH_4)(THF)$ (**4**)

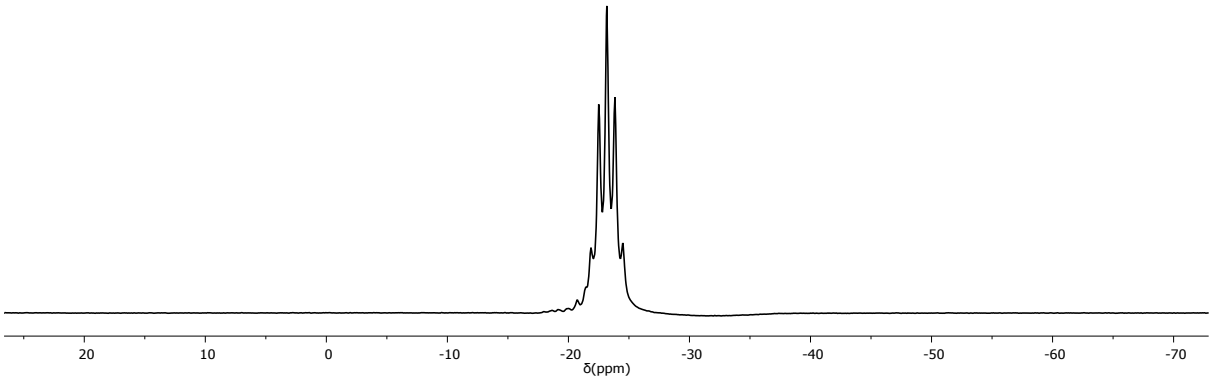

Fig. S12 ^{11}B NMR spectrum (C_6D_6, 128.4 MHz, 298 K) of $^{Me_2}SB(^{tBu}N,I^*)Sc(BH_4)(THF)$ (**4**).

IR spectrum of ^{Me_2}SB(^{tBu}N,I*)Sc(BH$_4$)(THF) (4)

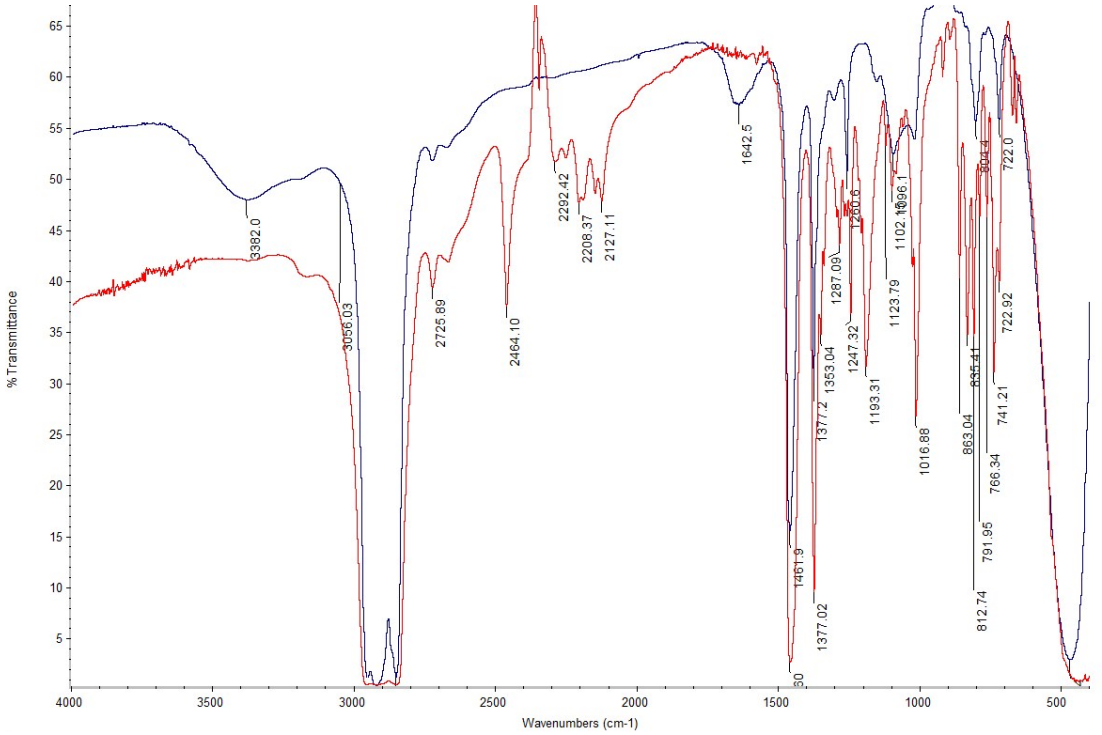

Fig. S13 IR spectra (NaCl plates, Nujol mull, cm^{-1}) of ^{Me_2}SB(^{tBu}N,I*)Sc(BH$_4$)(THF) (**4**, red) and nujol (blue).

Homonuclear decoupled $^{1}H\{^{1}H\}$ NMR spectra of PLA synthesised by the ROP of *L*- or *rac*-lactide using $^{Me}_{2}$SB($^{t\text{Bu}}$N,I*)Sc(Cl)(THF) (1).

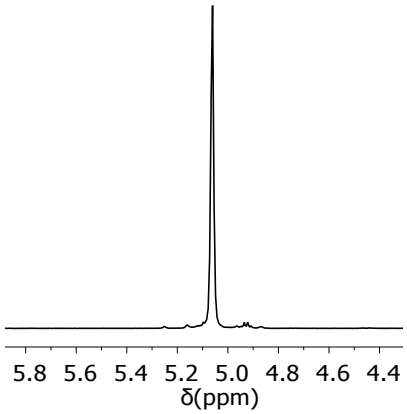

Fig. S14 $^{1}H\{^{1}H\}$ NMR spectrum ($CDCl_3$, 400.2 MHz, 298 K) of PLA synthesised from ROP of *L*-lactide with $^{Me}_{2}$SB($^{t\text{Bu}}$N,I*)Sc(Cl)(THF) (**1**). Conditions: $[L\text{-LA}]_0$:$[\mathbf{1}]_0$ = 100:1, $[L\text{-LA}]_0$ = 0.5 M, $[\mathbf{1}]_0$ = 0.005 M, 7.0 mL benzene at 70 °C.

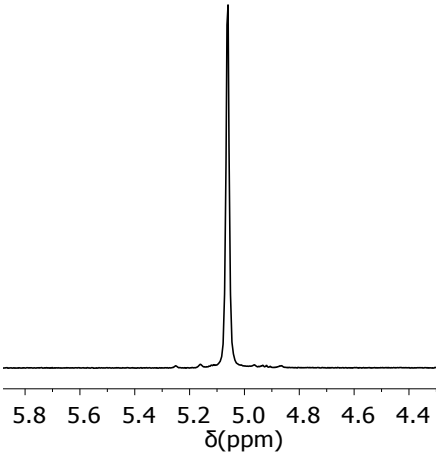

Fig. S15 $^{1}H\{^{1}H\}$ NMR spectrum ($CDCl_3$, 400.2 MHz, 298 K) of PLA synthesised from ROP of *L*-lactide with $^{Me}_{2}$SB($^{t\text{Bu}}$N,I*)Sc(Cl)(THF) (**1**) and benzyl alcohol (BnOH). Conditions: $[L\text{-LA}]_0$:$[\mathbf{1}]_0$:$[\text{BnOH}]_0$ = 100:1:1, $[L\text{-LA}]_0$ = 0.5 M, $[\mathbf{1}]_0$ = 0.005 M, 7.0 mL benzene at 70 °C.

Homonuclear decoupled $^{1}H\{^{1}H\}$ NMR spectra of PLA synthesised by the ROP of *L*- or *rac*-lactide using $^{Me_2}SB(^{tBu}N,I^*)Sc(O\text{-}2,6\text{-}^{i}Pr\text{-}C_6H_3)(THF)$ (2).

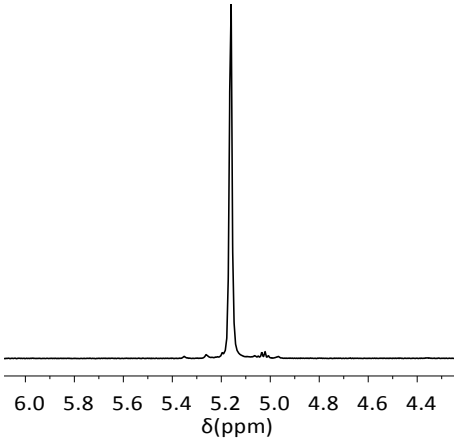

Fig. S16 $^{1}H\{^{1}H\}$ NMR spectrum ($CDCl_3$, 400.2 MHz, 298 K) of PLA synthesised from ROP of *L*-lactide with $^{Me_2}SB(^{tBu}N,I^*)Sc(O\text{-}2,6\text{-}^{i}Pr\text{-}C_6H_3)(THF)$ (**2**). Conditions: $[L\text{-LA}]_0$:$[\mathbf{2}]_0$ = 1000:1, $[L\text{-LA}]_0$ = 0.5 M, $[\mathbf{2}]_0$ = 0.0005 M, 7.0 mL benzene at 70 °C.

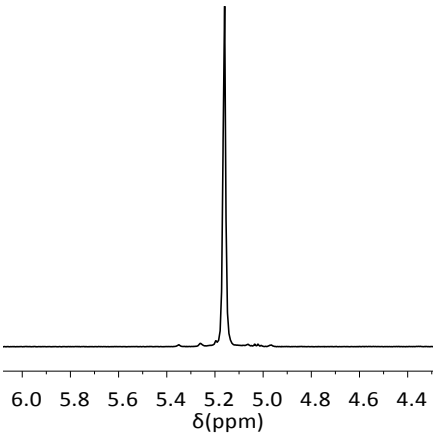

Fig. S17 $^{1}H\{^{1}H\}$ NMR spectrum ($CDCl_3$, 400.2 MHz, 298 K) of PLA synthesised from ROP of *L*-lactide with $^{Me_2}SB(^{tBu}N,I^*)Sc(O\text{-}2,6\text{-}^{i}Pr\text{-}C_6H_3)(THF)$ (**2**). Conditions: $[L\text{-LA}]_0$:$[\mathbf{2}]_0$ = 800:1, $[L\text{-LA}]_0$ = 0.5 M, $[\mathbf{2}]_0$ = 0.000625 M, 7.0 mL benzene at 70 °C.

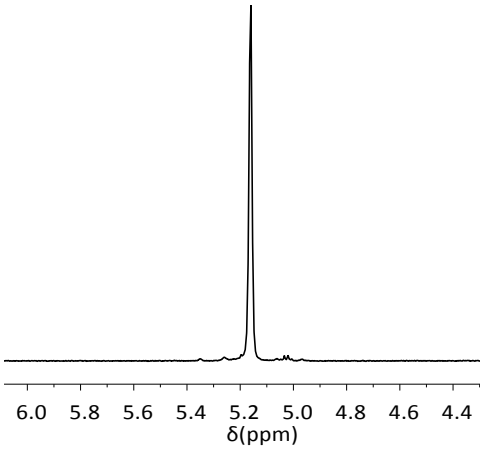

Fig. S18 $^{1}H\{^{1}H\}$ NMR spectrum ($CDCl_3$, 400.2 MHz, 298 K) of PLA synthesised from ROP of *L*-lactide with $^{Me}{}_2SB(^{tBu}N,I^*)Sc(O\text{-}2,6\text{-}^{i}Pr\text{-}C_6H_3)(THF)$ (**2**). Conditions: $[L\text{-LA}]_0$:$[\mathbf{2}]_0$ = 600:1, $[L\text{-LA}]_0$ = 0.5 M, $[\mathbf{2}]_0$ = 0.00083 M, 7.0 mL benzene at 70 °C.

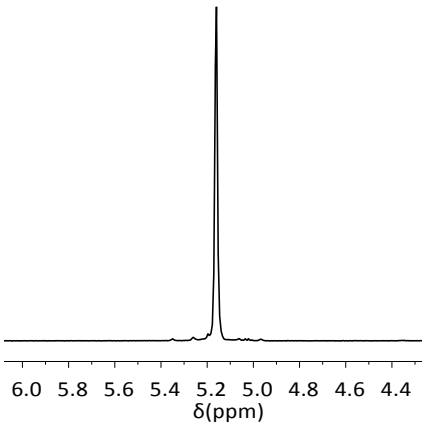

Fig. S19 $^{1}H\{^{1}H\}$ NMR spectrum ($CDCl_3$, 400.2 MHz, 298 K) of PLA synthesised from ROP of *L*-lactide with $^{Me}{}_2SB(^{tBu}N,I^*)Sc(O\text{-}2,6\text{-}^{i}Pr\text{-}C_6H_3)(THF)$ (**2**). Conditions: $[L\text{-LA}]_0$:$[\mathbf{2}]_0$ = 400:1, $[L\text{-LA}]_0$ = 0.5 M, $[\mathbf{2}]_0$ = 0.00125 M, 7.0 mL benzene at 70 °C.

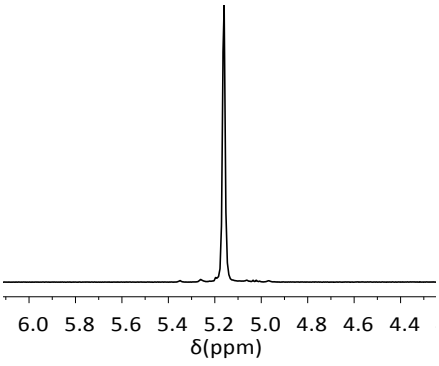

Fig. S20 $^{1}H\{^{1}H\}$ NMR spectrum ($CDCl_3$, 400.2 MHz, 298 K) of PLA synthesised from ROP of *L*-lactide with $^{Me}{}_2SB(^{tBu}N,I^*)Sc(O\text{-}2,6\text{-}^{i}Pr\text{-}C_6H_3)(THF)$ (**2**). Conditions: $[L\text{-LA}]_0$:$[\mathbf{2}]_0$ = 1000:1, $[L\text{-LA}]_0$ = 0.5 M, $[\mathbf{2}]_0$ = 0.0005 M, 7.0 mL benzene at 80 °C.

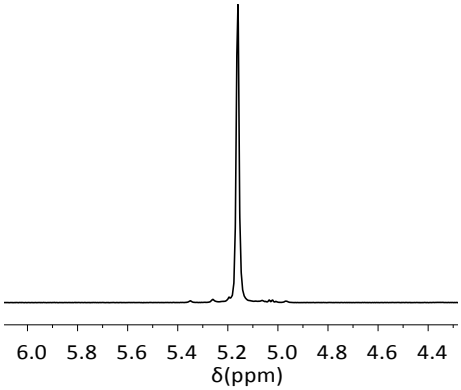

Fig. S21 $^{1}H\{^{1}H\}$ NMR spectrum ($CDCl_3$, 400.2 MHz, 298 K) of PLA synthesised from ROP of *L*-lactide with $^{Me_2}SB(^{tBu}N,I^*)Sc(O\text{-}2,6\text{-}^{i}Pr\text{-}C_6H_3)(THF)$ (**2**). Conditions: $[L\text{-LA}]_0:[\mathbf{2}]_0$ = 1000:1, $[L\text{-LA}]_0$ = 0.5 M, $[\mathbf{2}]_0$ = 0.0005 M, 7.0 mL benzene at 60 °C.

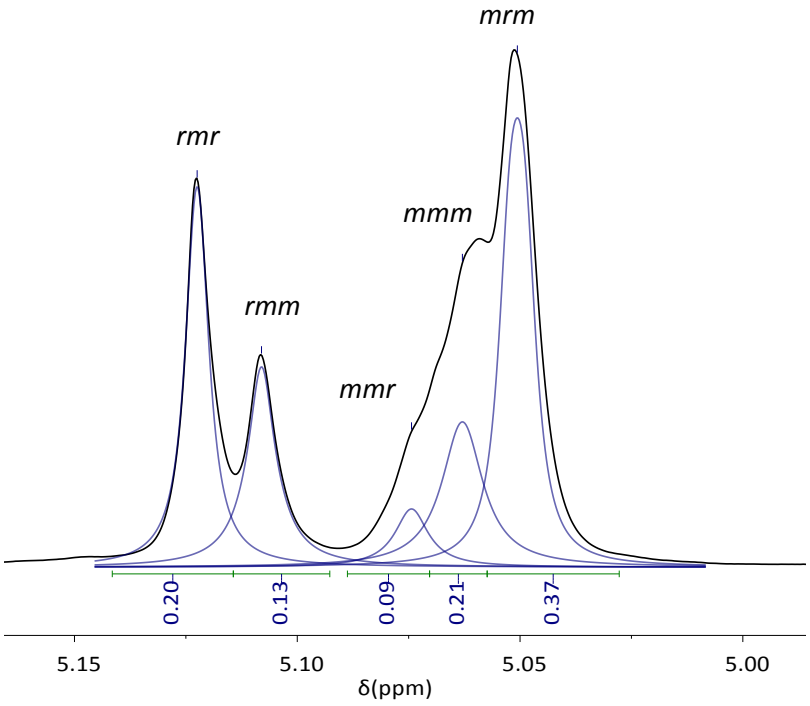

Fig. S22 $^{1}H\{^{1}H\}$ NMR spectrum ($CDCl_3$, 400.2 MHz, 298 K) of moderately heterotactic PLA (P_r =0.71) synthesised from ROP of *rac*-lactide with $^{Me_2}SB(^{tBu}N,I^*)Sc(O\text{-}2,6\text{-}^{i}Pr\text{-}C_6H_3)(THF)$ (**2**). Conditions: $[rac\text{-LA}]_0:[\mathbf{2}]_0$ = 1000:1, $[rac\text{-LA}]_0$ = 0.5 M, $[\mathbf{2}]_0$ = 0.0005 M, 7.0 mL benzene at 70 °C.

Tetrad	Probability	P_r (deconvolution)	P_r (integration)
rmr	$P_m^2/2$	0.70	0.65
mmm	$P_m^2 + (P_rP_m/2)$	0.73	0.67
mrm	$(P_r^2 + P_rP_m)/2$	0.69	0.80
Average P_r		P_r = 0.71 ± 0.02	P_r = 0.71 ± 0.08

Homonuclear decoupled $^{1}H\{^{1}H\}$ NMR spectra of PLA synthesised by the ROP of *L*- or *rac*-lactide using $^{Me_2}SB(^{tBu}N,I^*)Sc(O\text{-}2,4\text{-}^{t}Bu\text{-}C_6H_3)(THF)$ (3).

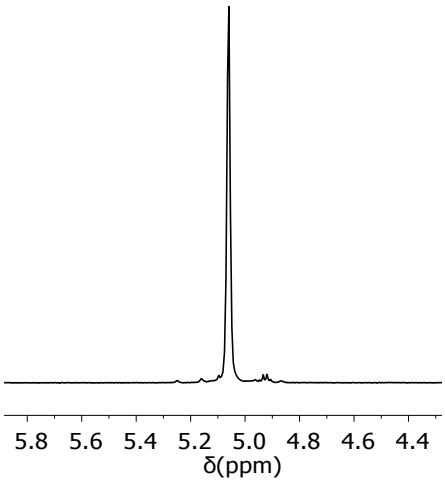

Figure S23 $^{1}H\{^{1}H\}$ NMR spectrum ($CDCl_3$, 400.2 MHz, 298 K) of PLA synthesised from ROP of *L*-lactide with $^{Me_2}SB(^{tBu}N,I^*)Sc(O\text{-}2,4\text{-}^{t}Bu\text{-}C_6H_3)(THF)$ (**3**). Conditions: $[L\text{-LA}]_0$:$[\mathbf{3}]_0$ = 1000:1, $[L\text{-LA}]_0$ = 0.5 M, $[\mathbf{3}]_0$ = 0.0005 M, 7.0 mL benzene at 70 °C.

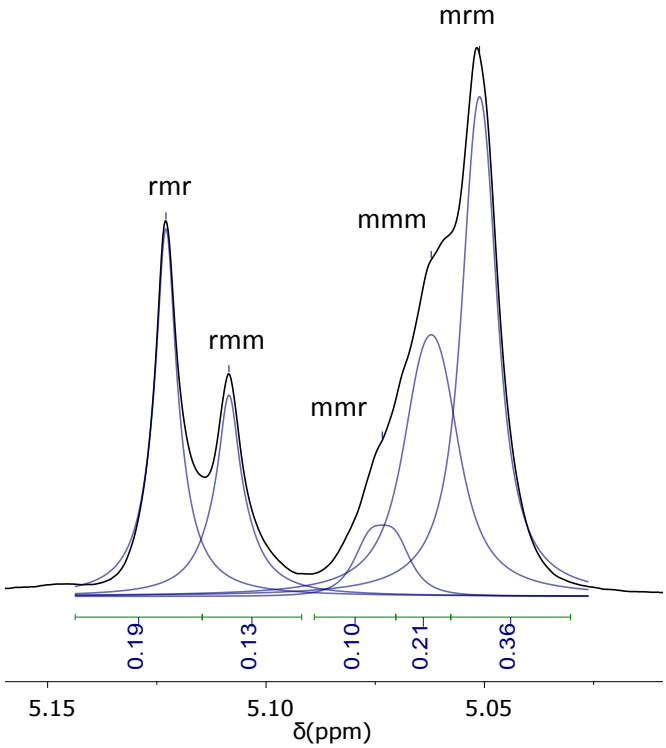

Figure S24 $^{1}H\{^{1}H\}$ NMR spectrum ($CDCl_3$, 400.2 MHz, 298 K) of moderately heterotactic PLA (P_r =0.65) synthesised from ROP of *rac*-lactide with $^{Me_2}SB(^{tBu}N,I^*)Sc(O\text{-}2,4\text{-}^{t}Bu\text{-}C_6H_3)(THF)$ (**3**). Conditions: $[rac\text{-LA}]_0$:$[\mathbf{3}]_0$ = 1000:1, $[rac\text{-LA}]_0$ = 0.5 M, $[\mathbf{3}]_0$ = 0.0005 M, 7.0 mL benzene at 70 °C.

Tetrad	Probability	P_r (deconvolution)	P_r (integration)
rmr	$P_m^2/2$	0.62	0.61
mmm	$P_m^2 + (P_rP_m/2)$	0.61	0.68
mrm	$(P_r^2 + P_rP_m)/2$	0.71	0.72
Average P_r		P_r = 0.65 ± 0.05	P_r = 0.67 ± 0.05

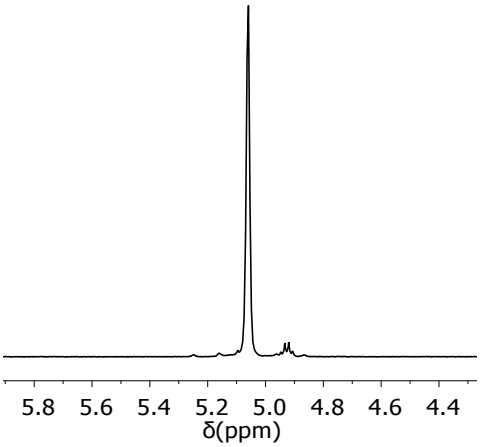

Figure S25 $^{1}H\{^{1}H\}$ NMR spectrum ($CDCl_3$, 400.2 MHz, 298 K) of PLA synthesised from ROP of *L*-lactide with $^{Me}_2$SB(^{tBu}N,I*)Sc(O-2,4-^{t}Bu-C_6H_3)(THF) (**3**). Conditions: $[L\text{-LA}]_0$:$[\mathbf{3}]_0$ = 1000:1, $[L\text{-LA}]_0$ = 0.5 M, $[\mathbf{3}]_0$ = 0.0005 M, 7.0 mL benzene at 60 °C.

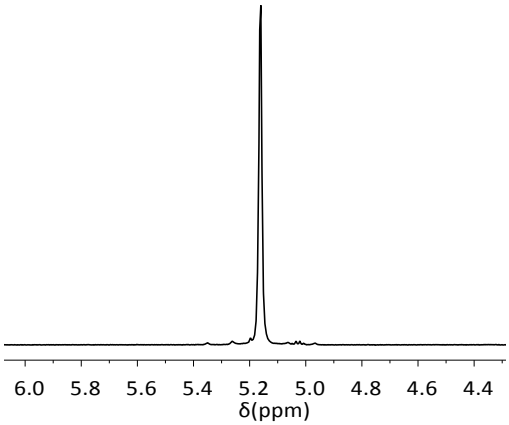

Figure S26 $^{1}H\{^{1}H\}$ NMR spectrum ($CDCl_3$, 400.2 MHz, 298 K) of PLA synthesised from ROP of *L*-lactide with $^{Me}_2$SB(^{tBu}N,I*)Sc(O-2,4-^{t}Bu-C_6H_3)(THF) (**3**). Conditions: $[L\text{-LA}]_0$:$[\mathbf{3}]_0$ = 1000:1, $[L\text{-LA}]_0$ = 0.5 M, $[\mathbf{3}]_0$ = 0.0005 M, 7.0 mL benzene at 50 °C.

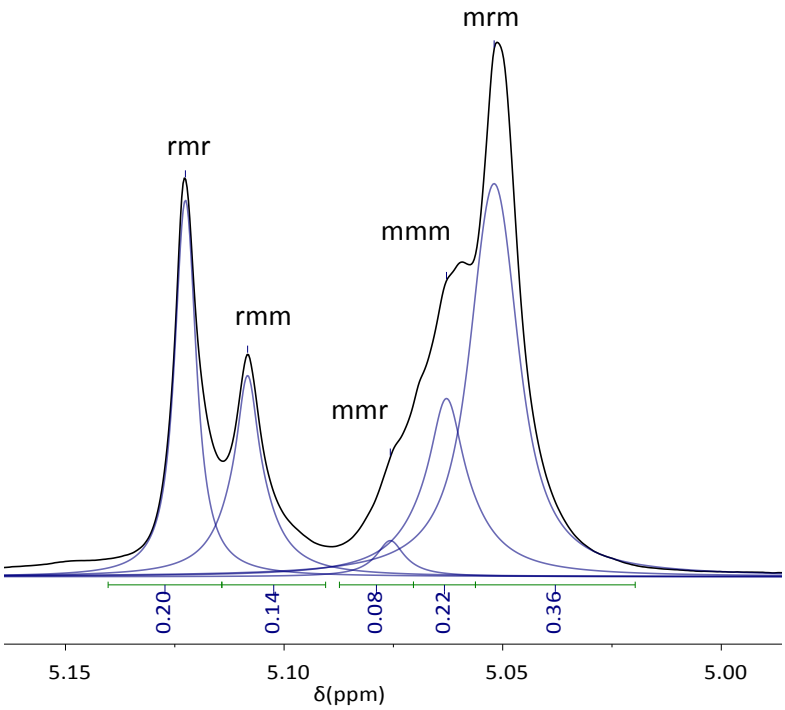

Figure S27 $^{1}H\{^{1}H\}$ NMR spectrum ($CDCl_3$, 400.2 MHz, 298 K) of moderately heterotactic PLA (P_r =0.72) synthesised from ROP of *rac*-lactide with $^{Me_2}SB(^{tBu}N,I^*)Sc(O\text{-}2,4\text{-}^{t}Bu\text{-}C_6H_3)(THF)$ (**3**). Conditions: $[rac\text{-LA}]_0:[\mathbf{3}]_0$ = 1000:1, $[rac\text{-LA}]_0$ = 0.5 M, $[\mathbf{3}]_0$ = 0.0005 M, 7.0 mL benzene at 50 °C.

Tetrad	Probability	P_r (deconvolution)	P_r (integration)
rmr	$P_m^2/2$	0.61	0.63
mmm	$P_m^2 + (P_rP_m/2)$	0.70	0.65
mrm	$(P_r^2 + P_rP_m)/2$	0.86	0.72
Average P_r		$P_r = 0.72 \pm 0.12$	$P_r = 0.67 \pm 0.05$

Homonuclear decoupled $^1H\{^1H\}$ NMR spectra of PLA synthesised by the ROP of *L*- or *rac*-lactide using $^{Me_2}SB(^{tBu}N,I^*)Sc(BH_4)(THF)$ (4).

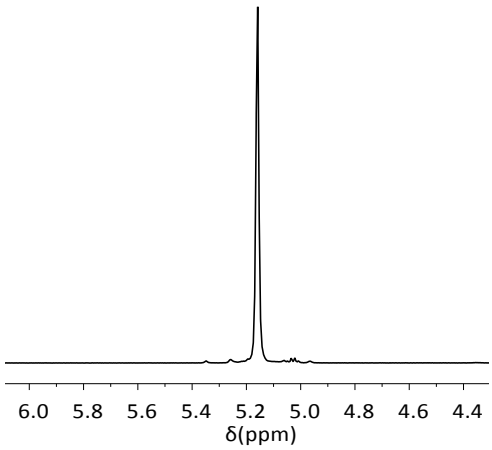

Fig. S28 $^1H\{^1H\}$ NMR spectrum ($CDCl_3$, 400.2 MHz, 298 K) of PLA synthesised from ROP of *L*-lactide with $^{Me_2}SB(^{tBu}N,I^*)Sc(BH_4)(THF)$ (**4**). Conditions: $[L\text{-LA}]_0$:$[\mathbf{4}]_0$ = 1000:1, $[L\text{-LA}]_0$ = 0.5 M, $[\mathbf{4}]_0$ = 0.0005 M, 7.0 mL benzene at 50 °C.

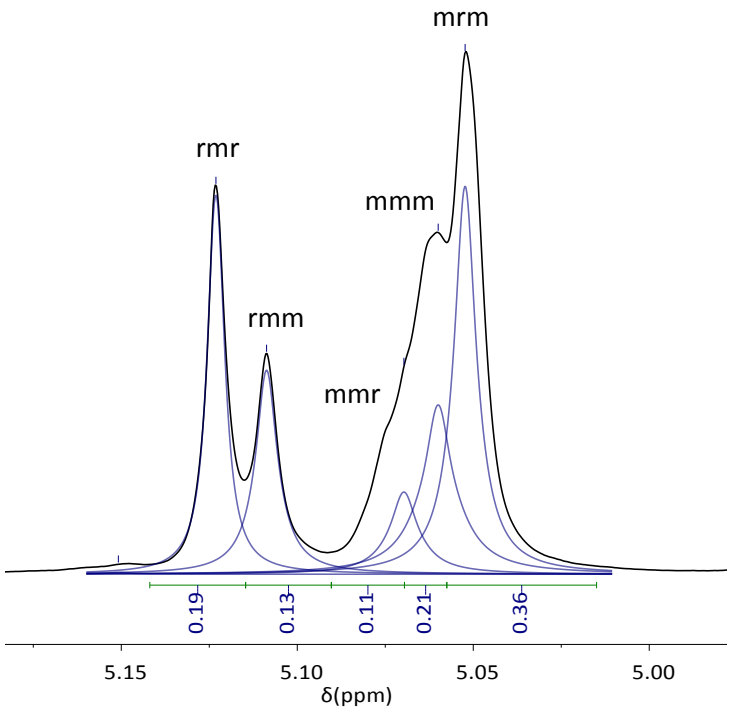

Fig. S29 $^1H\{^1H\}$ NMR spectrum ($CDCl_3$, 400.2 MHz, 298 K) of moderately heterotactic PLA (P_r =0.67) synthesised from ROP of *rac*-lactide with $^{Me_2}SB(^{tBu}N,I^*)Sc(BH_4)(THF)$ (**4**). Conditions: $[rac\text{-LA}]_0$:$[\mathbf{4}]_0$ = 1000:1, $[rac\text{-LA}]_0$ = 0.5 M, $[\mathbf{4}]_0$ = 0.0005 M, 7.0 mL benzene at 50 °C.

Tetrad	Probability	P_r (deconvolution)	P_r (integration)
rmr	$P_m^2/2$	0.68	0.62
mmm	$P_m^2 + (P_rP_m/2)$	0.69	0.68
mrm	$(P_r^2 + P_rP_m)/2$	0.64	0.72
Average P_r		P_r = 0.67 ± 0.05	P_r = 0.67 ± 0.03

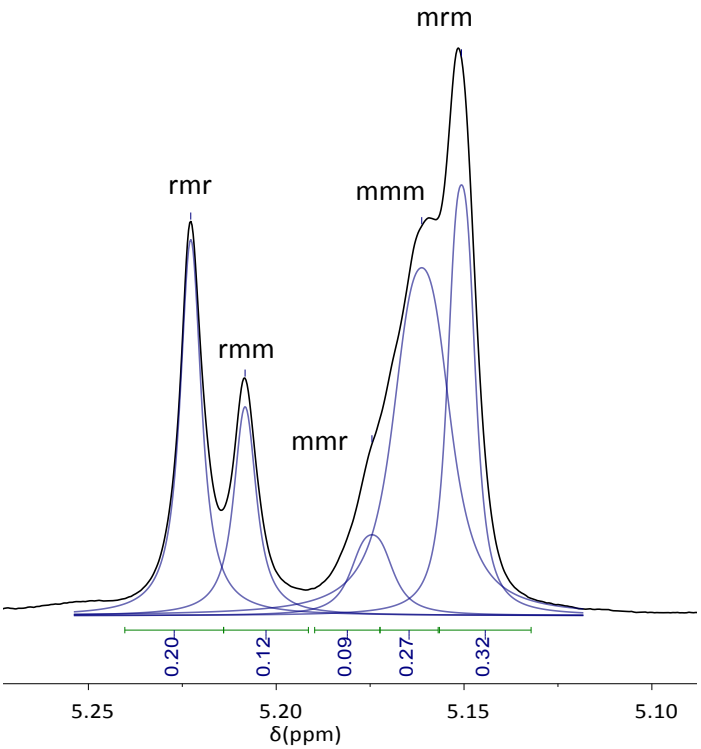

Fig. S30 $^{1}H\{^{1}H\}$ NMR spectrum ($CDCl_3$, 400.2 MHz, 298 K) of moderately heterotactic PLA (P_r =0.61) synthesised from ROP of *rac*-lactide with $^{Me}_2SB(^{tBu}N,I^*)Sc(BH_4)(THF)$ (**4**). Conditions: $[rac\text{-LA}]_0$:$[\mathbf{4}]_0$ = 1000:1, $[rac\text{-LA}]_0$ = 0.5 M, $[\mathbf{4}]_0$ = 0.0005 M, 7.0 mL benzene at 60 °C.

Tetrad	Probability	P_r (deconvolution)	P_r (integration)
rmr	$P_m^2/2$	0.54	0.63
mmm	$P_m^2 + (P_rP_m/2)$	0.72	0.61
mrm	$(P_r^2 + P_rP_m)/2$	0.60	0.64
Average P_r		P_r = 0.61 ± 0.10	P_r = 0.63 ± 0.01

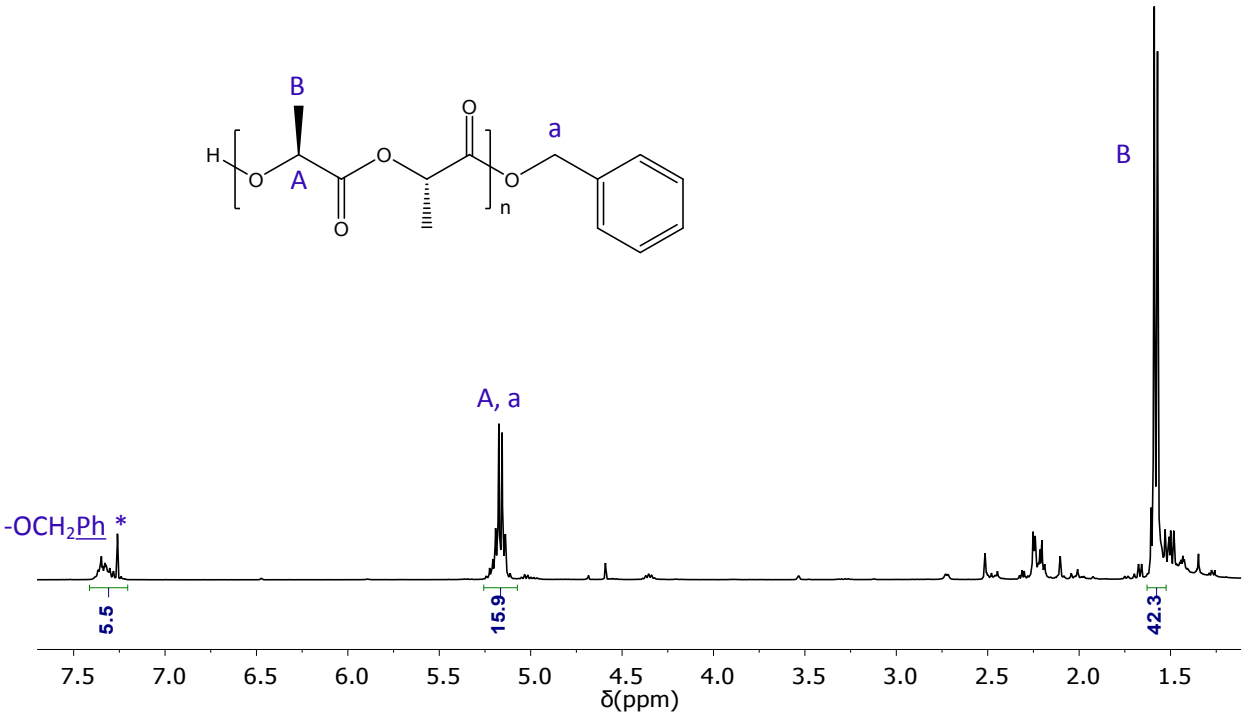

Fig. S31 ^{1}H NMR spectrum ($CDCl_3$, 400.2 MHz, 298 K) of PLA synthesised by ^{Me_2}SB($^{t\text{Bu}}$N,I*)Sc(Cl)(THF) (**1**) with benzyl alcohol. Conditions: [*L*-LA]$_0$:[**1**]$_0$:[BnOH]$_0$ = 10:1:1, [*L*-LA]$_0$ = 0.5 M, 0.7 mL benzene at 70 °C for 15 minutes. "*" denotes residual protio-solvent.

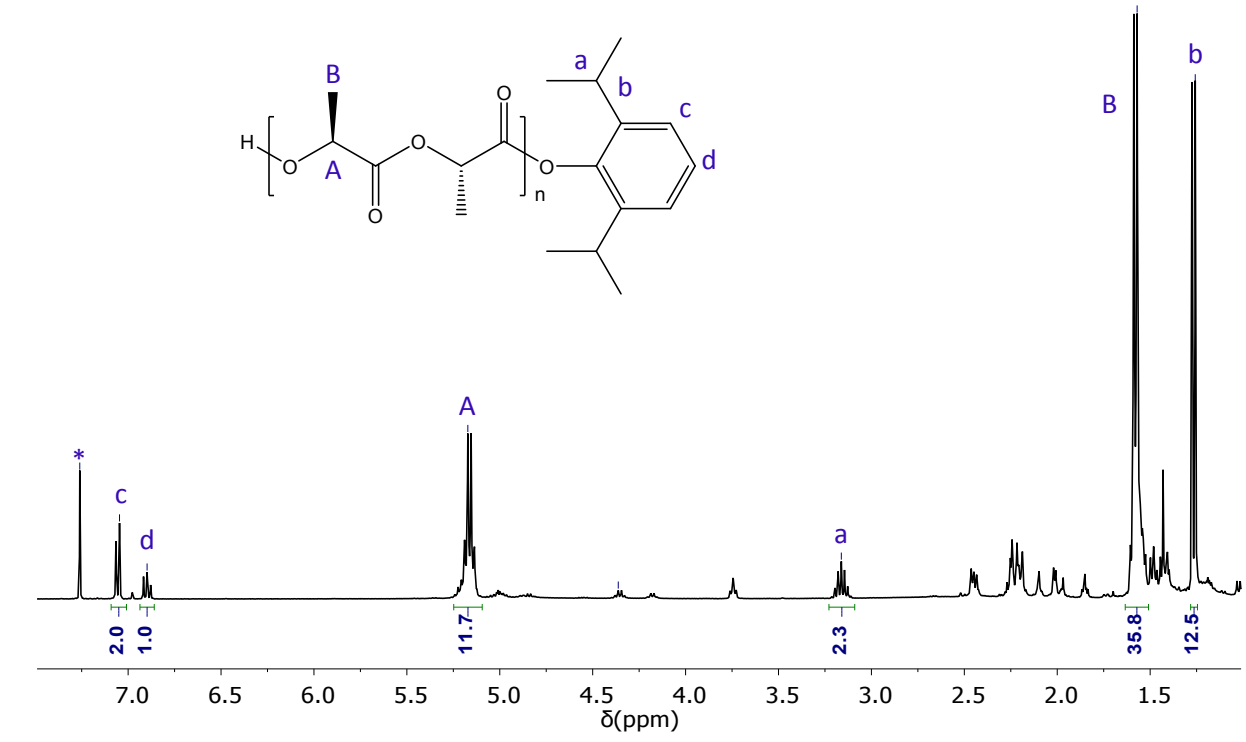

Fig. S32 ^{1}H NMR spectrum ($CDCl_3$, 400.2 MHz, 298 K) of PLA synthesised by ^{Me_2}SB($^{t\text{Bu}}$N,I*)Sc(O-2,6-^{i}Pr-C_6H_3)(THF) (**2**). Conditions: [*L*-LA]$_0$:[**2**]$_0$ = 10:1, [*L*-LA]$_0$ = 0.5 M, 0.7 mL benzene at 70 °C for 2 h. "*" denotes residual protio-solvent.

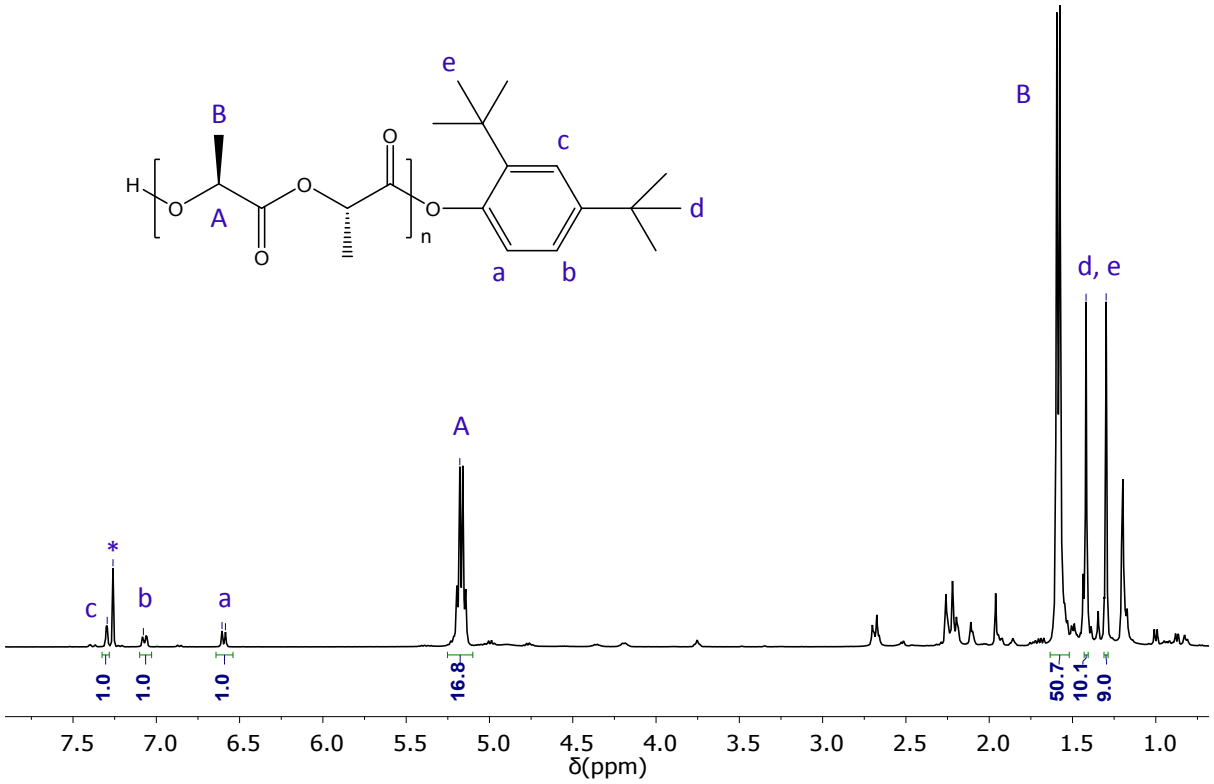

Fig. S33 ^{1}H NMR spectrum ($CDCl_3$, 400.2 MHz, 298 K) of PLA synthesised by ^{Me_2}SB($^{t\text{Bu}}$N,I*)Sc(O-2,4-^{t}Bu-C_6H_3)(THF) (**3**). Conditions: [*L*-LA]$_0$:[**3**]$_0$ = 10:1, [*L*-LA]$_0$ = 0.5 M, 0.7 mL benzene at 70 °C for 15 minutes. "*" denotes residual protio-solvent.

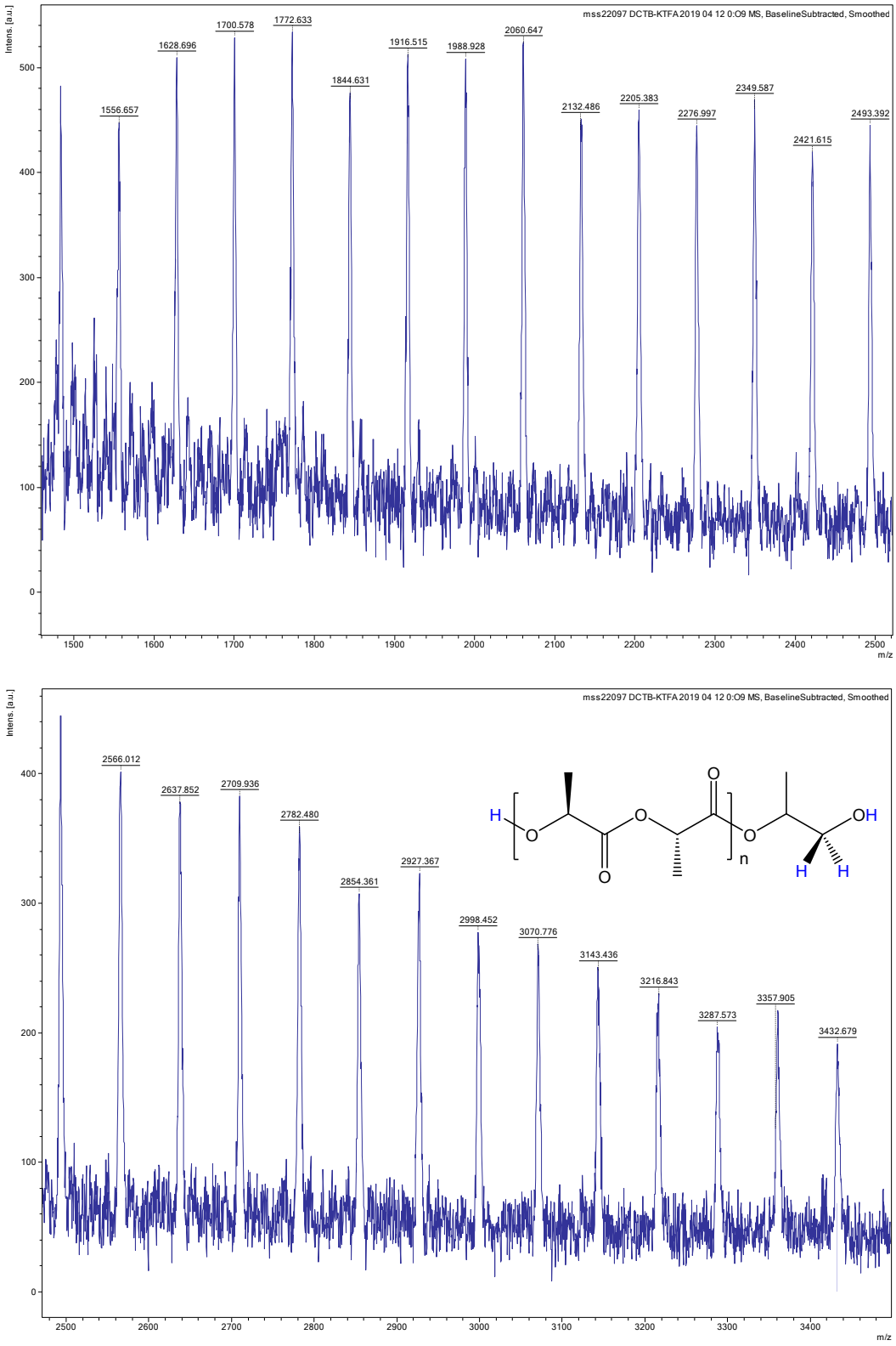

Fig. S34 and S35 MALDI-ToF mass spectra of PLA synthesised using ^{Me2}SB(^{tBu}N,I*)Sc(BH$_4$)(THF) (**4**). M_n(GPC) = 3790 g mol^{-1}, M_w/M_n = 1.35. Conditions: [*L*-LA]$_0$:[**4**]$_0$ = 20:1, [*L*-LA]$_0$ = 0.5 M, [**3**]$_0$ = 0.025 M, 0.7 mL benzene at 50 °C. The cationisation agent was KTFA, and the matrix was DCTB. Δ*m*/*z* = 72.0 Da between peak envelopes. Peak envelope centred at 1916.5 Da corresponds to PLA terminated with -OH and -CHMeCH$_2$OH end groups with 13 units of LA and K$^+$ [144.1(13) + 4 + 39.1 = 1916.4].

Additional crystallographic data

X-ray data collection and processing parameters

Single crystal X-ray diffraction data collection and structure determinations were performed by Dr Zoë Turner (University of Oxford). Crystals were mounted on MiTeGen MicroMounts using perfluoropolyether oil and rapidly transferred to a goniometer head on a diffractometer fitted with an Oxford Cryosystems Cryostream open-flow nitrogen cooling device.[4] Data collections were carried out at 150 K using an Oxford Diffraction Supernova diffractometer using mirror-monochromated Cu Kα radiation (λ = 1.54178 Å) and the data was processed using CrysalisPro.[5] The structures were solved using direct methods (SIR-92)[6] or a charge flipping algorithm (SUPERFLIP)[7] and refined by full-matrix least-squares procedures using the Win-GX software suite.[8] The ring slip parameter or $\Delta_{M\text{-}C}$ value indicates degree of distortion from η^5 bonding to η^3 bonding, and a good measurement for the indenyl effect.[9] The $\Delta_{M\text{-}C}$ value is calculated from Equation S1.

$$\Delta M - C = \left(\frac{C(8) + C(9)}{2}\right) - \left(\frac{C(1) + C(2) + C(3)}{3}\right)$$

Equation S1 $\Delta_{M\text{-}C}$ (Å) where C(#) denotes the Sc-C(#) bond length

Table S1 Selected metrical data for for $^{Me}_2$SB($^{t\text{Bu}}$N,I*)Sc(O-2,6-^{i}Pr-C_6H_3)(THF) (**2**), $^{Me}_2$SB($^{t\text{Bu}}$N,I*)Sc(O-2,4-^{t}Bu-C_6H_3)(THF) (**3**) and $^{Me}_2$SB($^{t\text{Bu}}$N,I*)Sc(BH_4)(THF) (**4**).

Complex	**2**	**3**	**4**
Sc-Cp_{cent} (Å)	2.1718(1)	2.1768(1)	2.1631(1)
Sc-OAr (Å)	1.9450(9)	1.9324(1)	-
Sc-O(THF) (Å)	2.1686(1)	2.1724(1)	2.1640(10)
Sc-N (Å)	2.0593(11)	2.0546(1)	2.0535(11)
Sc-Si (Å)	2.9858(1)	2.9787(1)	2.9555(1)
Sc-B (Å)	-	-	2.3572(16)
N-CMe_3 (Å)	1.4780(17)	1.482(2)	1.4845(17)
Sc-O-C(OAr) (°)	175.63(9)	152.93(11)	-
Cp_{cent}-Sc-OAr (°)	119.70(1)	120.07(1)	-
Cp_{cent}-Sc-O(THF) (°)	112.56(1)	114.83(1)	113.56(1)
Cp_{cent}-Sc-N (°)	103.99(1)	104.06(1)	104.70(1)
OAr-Sc-O(THF)	102.13(1)	100.40(1)	-
OAr-Sc-N	116.88(1)0	111.86(1)	-
$\Delta_{M\text{-}C}$ (Å)	0.0892	0.0898	0.07845

Table S2 Selected crystallographic data for ^{Me2}SB(^{tBu}N,I*)Sc(O-2,6-^{i}Pr-C_6H_3)(THF) (**2**), ^{Me2}SB(^{tBu}N,I*)Sc(O-2,4-^{t}Bu-C_6H_3)(THF) (**3**) and ^{Me2}SB(^{tBu}N,I*)Sc(BH_4)(THF) (**4**).

Complex	**2**	**3**	**4**
		Crystal data	
Chemical formula	$C_{37}H_{58}NO_2ScSi$	$C_{39}H_{62}NO_2ScSi$	$C_{25}H_{45}BNOScSi$
M_r	621.89	649.94	459.48
Crystal system, space group	Monoclinic, $P2_1/n$	Monoclinic, $P2_1/c$	Monoclinic, $P2_1/c$
Temperature (K)	150	150	150
a, b, c (Å)	11.8504 (1), 16.9140 (2), 18.1946 (2)	8.8421 (1), 17.8213 (2), 24.1749 (4)	8.6950 (1), 18.2950 (2), 17.0861 (2)
α, β, γ (°)	90, 103.479 (1), 90	90, 96.886 (1), 90	90, 103.545 (1), 90
V (Å^3)	3546.43 (7)	3781.95 (9)	2462.37 (5)
Z	4	4	4
Density (g cm^{-3})	1.165	1.141	1.155
Radiation type	Cu $K\alpha$	Cu $K\alpha$	Cu $K\alpha$
μ (mm^{-1})	2.325	2.200	2.916
Crystal size (mm)	0.078, 0.114, 0.171	0.040, 0.132, 0.290	0.144, 0.208, 0.321
		Data collection	
Diffractometer	SuperNova, Dual, Cu at home/near, Atlas	Supernova, Dual, Cu at home/near, Atlas	Supernova, Dual, Cu at home/near, Atlas
Absorption correction	Multi-scan *CrysAlisPro* 1.171.39.46 (Rigaku Oxford Diffraction, 2018) Empirical absorption correction using spherical harmonics, implemented in SCALE3 ABSPACK	Gaussian *CrysAlisPro* 1.171.39.46 (Rigaku Oxford Diffraction, 2018) Numerical absorption correction based on gaussian integration over a multifaceted crystal	Multi-scan *CrysAlisPro* 1.171.39.46 (Rigaku Oxford Diffraction, 2018) Empirical absorption correction using spherical harmonics, implemented in SCALE3 ABSPACK

	scaling algorithm.	model Empirical absorption correction using spherical harmonics, implemented in SCALE3 ABSPACK scaling algorithm.	scaling algorithm
T_{min}, T_{max}	0.810, 1.000	0.608, 1.000	0.839, 1.000
No. of measured, independent and observed [$I > 2\sigma(I)$] reflections	27961, 7391, 6718	35204, 7725, 6791	21867, 5406, 5189
R_{int}	0.0259	0.0306	0.0194
Refinement			
$R[F^2 > 2\sigma(F^2)]$, $wR(F^2)$, S	0.0327, 0.0912, 1.050	0.0387, 0.1107, 1.035	0.0293, 0.0925, 0.883
No. of reflections	7391	7725	5406
No. of parameters	413	445	298
No. of restraints	0	7	0
$(\Delta/\sigma)_{max}$	0.001	0.001	0.002
$\Delta\rho_{max}$, $\Delta\rho_{min}$ (e Å^{-3})	0.298, -0.358	0.293, –0.372	0.272, –0.240

Additional polymerisation data

Table S3 ROP of *L*-LA using ^{Me_2}SB(^{tBu}N,I*)Sc(Cl)(THF) (**1**) with [*L*-LA]$_0$:[**1**]$_0$ = 100:1.[a]

Time (h)	Conversion 1 (%)[b]	Time (h)	Conversion 2 (%)[b]
1.00	20	1.00	16
2.00	44	2.00	42
2.50	57	2.50	50
3.00	65	3.00	61
3.50	72	3.50	69
4.00	79	4.00	75
4.50	84	4.50	80
5.00	86	5.00	84
		6.00	90
k_{obs} = 0.45 ± 0.02 h^{-1}. R^2 = 0.993		k_{obs} = 0.43 ± 0.01 h^{-1}. R^2 = 0.994	

[a]Conditions: [*L*-LA]$_0$:[**1**]$_0$ = 100:1, [*L*-LA]$_0$ = 0.5 M, [**1**]$_0$ = 0.005 M, 7.0 mL benzene at 70 °C. Aliquots were taken at given intervals. [b]Measured by ^{1}H NMR spectroscopic analyses.

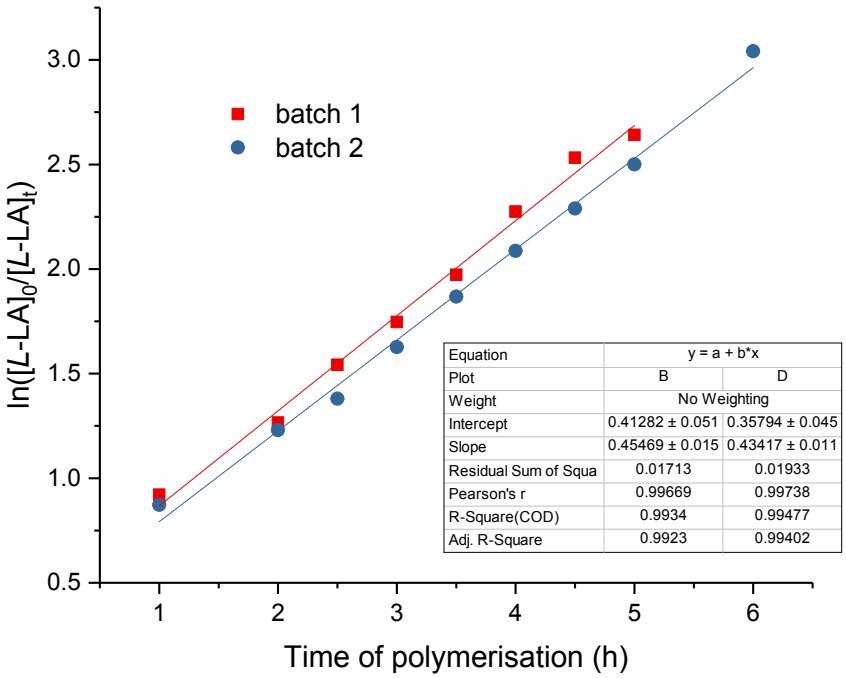

Fig. S36 plots of ln([*L*-LA]$_0$/[*L*-LA]$_t$) *vs.* time. Red squares: batch 1 (k_{obs} = 0.45 ± 0.02 h^{-1}. R^2 = 0.993), Blue circles: batch 2 (k_{obs} = 0.43 ± 0.01 h^{-1}. R^2 = 0.994). Conditions: [*L*-LA]$_0$:[**1**]$_0$ = 100:1, [*L*-LA]$_0$ = 0.5 M, [**1**]$_0$ = 0.005 M, 7.0 mL benzene at 70 °C.

Table S4 ROP of *L*-LA using $^{Me}_2$SB(^{tBu}N,I*)Sc(Cl)(THF) (**1**) and benzyl alcohol with $[L\text{-LA}]_0$:$[\mathbf{1}]_0$:$[\text{BnOH}]_0$ = 100:1:1.[a]

Time (h)	Conversion 1 (%)[b]	Time (h)	Conversion 2 (%)[b]
0.33	55	0.17	27
0.50	76	0.25	45
0.67	87	0.33	63
0.83	93	0.50	79
		0.67	90
		0.83	94
k_{obs} = 3.72 ± 0.04 h^{-1}. R^2 = 0.999		k_{obs} = 3.85 ± 0.01 h^{-1}. R^2 = 0.996	

[a]Conditions: $[L\text{-LA}]_0$:$[\mathbf{1}]_0$:$[\text{BnOH}]_0$ = 100:1:1, $[L\text{-LA}]_0$ = 0.5 M, $[\mathbf{1}]_0$ = 0.005 M, 7.0 mL benzene at 70 °C. Aliquots were taken at given intervals. [b]Measured by ^{1}H NMR spectroscopic analyses.

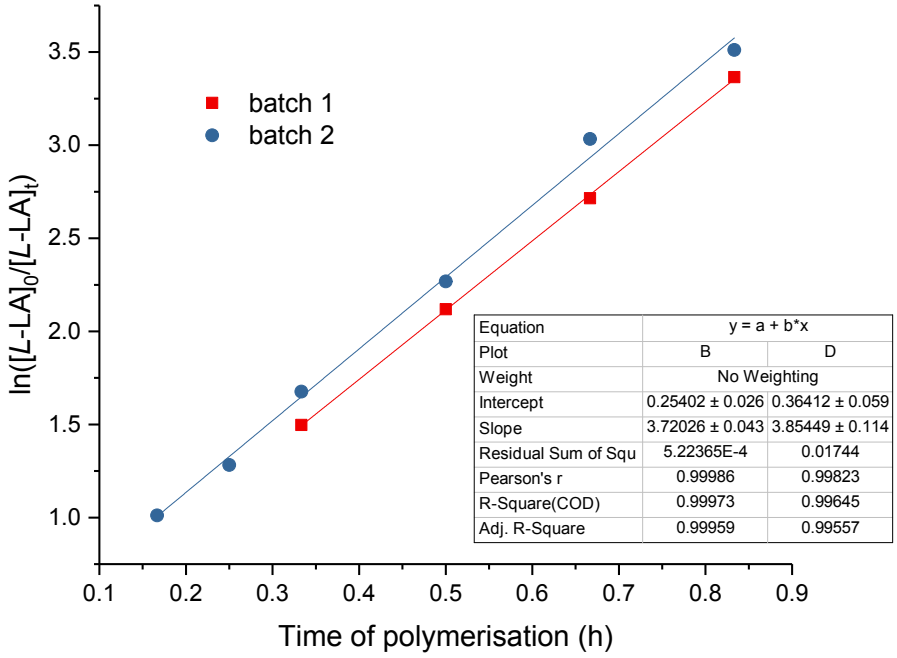

Fig. S37 plots of $\ln([L\text{-LA}]_0/[L\text{-LA}]_t)$ *vs.* time. Red squares: batch 1 (k_{obs} = 3.72 ± 0.04 h^{-1}. R^2 = 0.999), Blue circles: batch 2 (k_{obs} = 3.85 ± 0.01 h^{-1}. R^2 = 0.996). Conditions: $[L\text{-LA}]_0$:$[\mathbf{1}]_0$:$[\text{BnOH}]_0$ = 100:1:1, $[L\text{-LA}]_0$ = 0.5 M, $[\mathbf{1}]_0$ = 0.005 M, 7.0 mL benzene at 70 °C.

Table S5 ROP of *L*-LA using $^{Me}_2$SB(^{tBu}N,I*)Sc(O-2,6-^{i}Pr-C_6H_3)(THF) (**2**) with $[L\text{-LA}]_0$:$[\mathbf{2}]_0$ = 1000:1.[a]

Time (h)	Conversion 1 (%)[b]	Time (h)	Conversion 2 (%)[b]
0.25	6	0.25	6
0.50	11	0.50	10
0.75	20	0.75	18
1.00	29	1.00	28
1.25	40	1.25	36
1.50	49	1.50	46
1.75	59	1.75	54
2.00	67	2.00	61
2.25	73	2.25	68
2.50	78	2.50	74
2.75	81	2.75	78
3.00	84	3.00	81
3.25	86	3.25	85
3.50	88	3.50	86
3.75	90	3.75	88
		4.00	90
k_{obs} = 0.70 ± 0.01 h^{-1}. R^2 = 0.996		k_{obs} = 0.66 ± 0.01 h^{-1}. R^2 = 0.996	
M_n = 92 100 g mol^{-1}		M_n = 111 160 g mol^{-1}	
M_w/M_n = 1.14		M_w/M_n = 1.12	

[a]Conditions: $[L\text{-LA}]_0$:$[\mathbf{2}]_0$ = 1000:1, $[L\text{-LA}]_0$ = 0.5 M, $[\mathbf{2}]_0$ = 0.0005 M, 7.0 mL benzene at 70 °C. Aliquots were taken at given intervals. [b]Measured by ^{1}H NMR spectroscopic analyses.

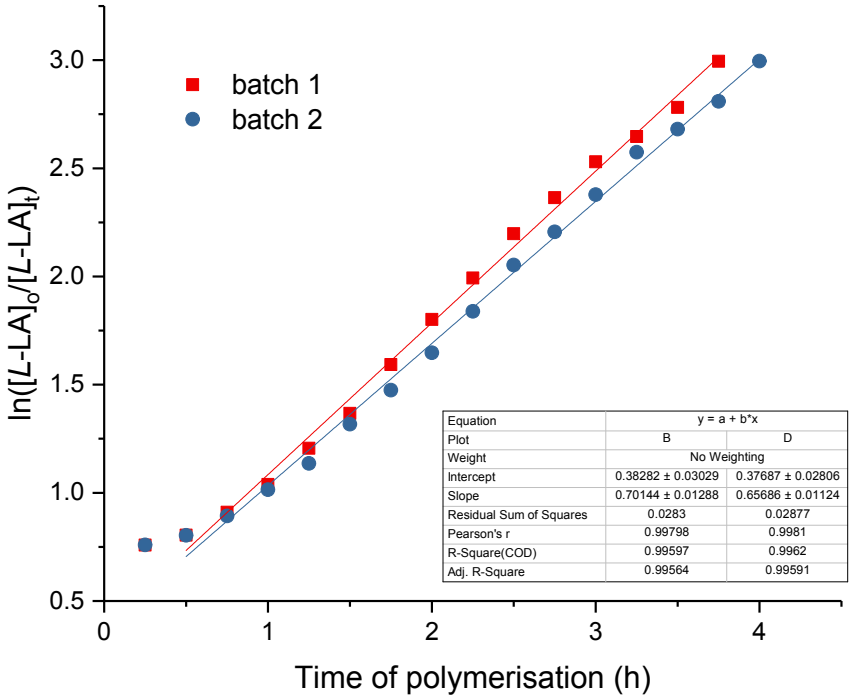

Fig. S38 plots of $\ln([L\text{-LA}]_0/[L\text{-LA}]_t)$ *vs.* time. Red squares: batch 1 (k_{obs} = 0.70 ± 0.01 h^{-1}. R^2 = 0.996), Blue circles: batch 2 (k_{obs} = 0.66 ± 0.01 h^{-1}. R^2 = 0.996). Conditions: $[L\text{-LA}]_0$:$[\mathbf{2}]_0$ = 1000:1, $[L\text{-LA}]_0$ = 0.5 M, $[\mathbf{2}]_0$ = 0.0005 M, 7.0 mL benzene at 70 °C.

Table S6 ROP of *L*-LA using ^{Me2}SB(^{tBu}N,I*)Sc(O-2,6-^{i}Pr-C_6H_3)(THF) (**2**) with $[L\text{-LA}]_0$:$[\mathbf{2}]_0$ = 800:1.[a]

Time (h)	Conversion 1 (%)[b]	Time (h)	Conversion 2 (%)[b]
0.25	7	0.25	7
0.50	13	0.50	12
0.75	22	0.75	23
1.00	33	1.00	38
1.25	45	1.25	50
1.50	55	1.50	61
1.75	65	1.75	70
2.00	72	2.00	76
2.25	77	2.25	80
2.50	83	2.50	86
2.75	86	2.75	89
3.00	89	3.00	90
k_{obs} = 0.82 ± 0.03 h^{-1}. R^2 = 0.985		k_{obs} = 0.88 ± 0.03 h^{-1}. R^2 = 0.991	
M_n = 82 290 g mol^{-1}		M_n = 87 810 g mol^{-1}	
M_w/M_n = 1.13		M_w/M_n = 1.12	

[a]Conditions: $[L\text{-LA}]_0$:$[\mathbf{2}]_0$ = 800:1, $[L\text{-LA}]_0$ = 0.5 M, $[\mathbf{2}]_0$ = 0.000625 M, 7.0 mL benzene at 70 °C. Aliquots were taken at given intervals. [b]Measured by ^{1}H NMR spectroscopic analyses.

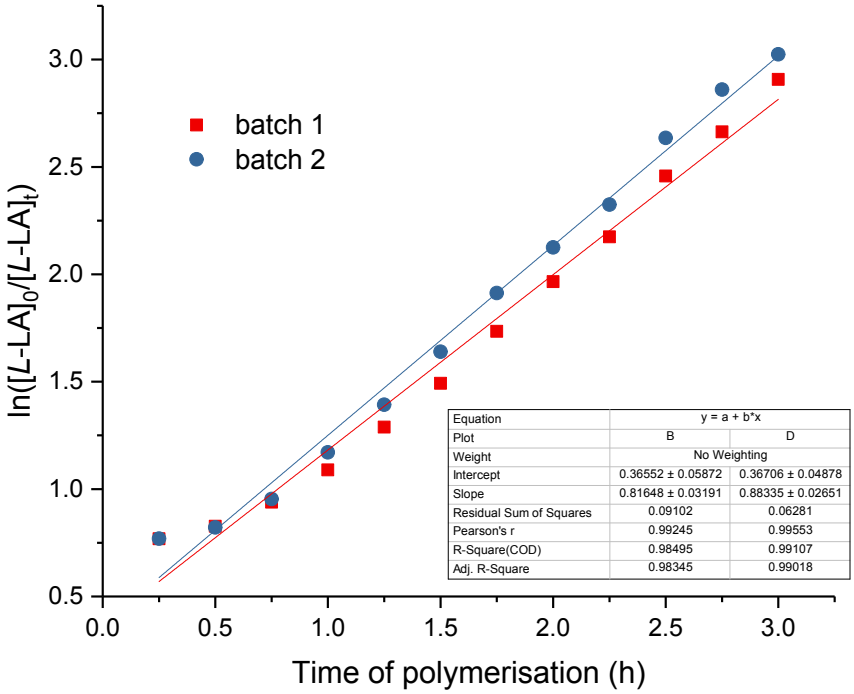

Fig. S39 plots of $\ln([L\text{-LA}]_0/[L\text{-LA}]_t)$ *vs.* time. Red squares: batch 1 (k_{obs} = 0.82 ± 0.03 h^{-1}. R^2 = 0.985), Blue circles: batch 2 (k_{obs} = 0.88 ± 0.03 h^{-1}. R^2 = 0.991). Conditions: $[L\text{-LA}]_0$:$[\mathbf{2}]_0$ = 800:1, $[L\text{-LA}]_0$ = 0.5 M, $[\mathbf{2}]_0$ = 0.000625 M, 7.0 mL benzene at 70 °C.

Table S7 ROP of *L*-LA using $^{Me}_2$SB(^{tBu}N,I*)Sc(O-2,6-^{i}Pr-C_6H_3)(THF) (**2**) with $[L\text{-LA}]_0$:$[\mathbf{2}]_0$ = 600:1.[a]

Time (h)	Conversion 1 (%)[b]	Time (h)	Conversion 2 (%)[b]
0.25	9	0.25	9
0.50	14	0.50	14
0.75	26	0.75	24
1.00	42	1.00	39
1.25	59	1.25	52
1.50	70	1.50	64
1.75	79	1.75	73
2.00	83	2.00	80
2.25	87	2.25	85
2.50	90	2.50	88
2.75	93	2.75	89
3.00	93	3.00	91
k_{obs} = 1.07 ± 0.04 h^{-1}. R^2 = 0.988		k_{obs} = 1.00 ± 0.03 h^{-1}. R^2 = 0.993	
M_n = 68 220 g mol^{-1}		M_n = 86 870 g mol^{-1}	
M_w/M_n = 1.14		M_w/M_n = 1.13	

[a]Conditions: $[L\text{-LA}]_0$:$[\mathbf{2}]_0$ = 600:1, $[L\text{-LA}]_0$ = 0.5 M, $[\mathbf{2}]_0$ = 0.00083 M, 7.0 mL benzene at 70 °C. Aliquots were taken at given intervals. [b]Measured by ^{1}H NMR spectroscopic analyses.

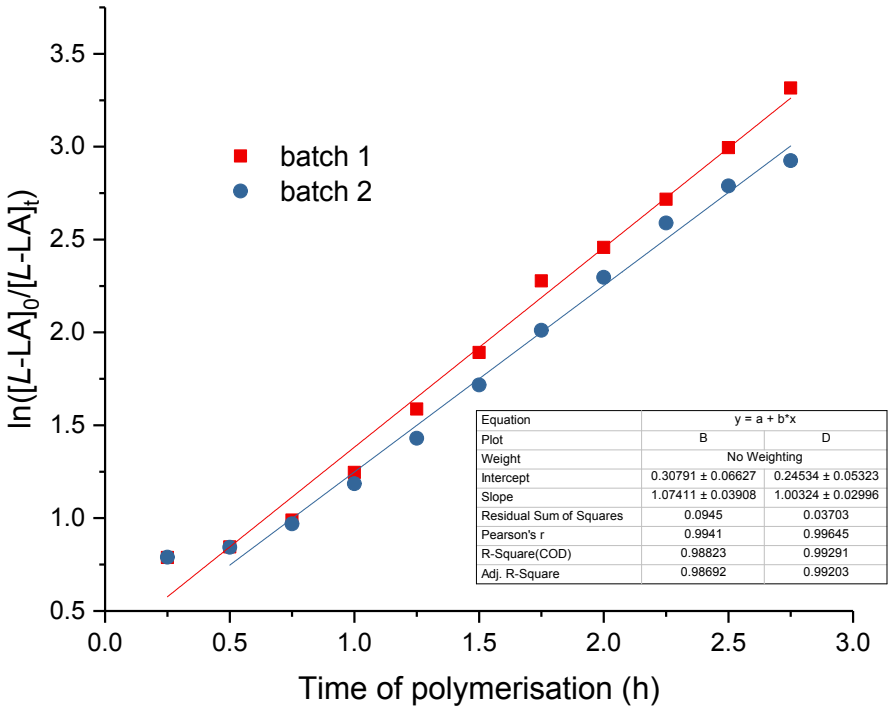

Fig. S40 plots of $\ln([L\text{-LA}]_0/[L\text{-LA}]_t)$ *vs.* time. Red squares: batch 1 (k_{obs} = 1.07 ± 0.04 h^{-1}. R^2 = 0.988), Blue circles: batch 2 (k_{obs} = 1.00 ± 0.03 h^{-1}. R^2 = 0.993). Conditions: $[L\text{-LA}]_0$:$[\mathbf{2}]_0$ = 600:1, $[L\text{-LA}]_0$ = 0.5 M, $[\mathbf{2}]_0$ = 0.00083 M, 7.0 mL benzene at 70 °C.

Table S8 ROP of *L*-LA using ^{Me_2}SB(^{tBu}N,I*)Sc(O-2,6-^{i}Pr-C_6H_3)(THF) (**2**) with [*L*-LA]$_0$:[**2**]$_0$ = 400:1.[a]

Time (h)	Conversion 1 (%)[b]	Time (h)	Conversion 2 (%)[b]
0.33	13	0.25	10
0.67	23	0.50	17
1.00	45	0.75	27
1.25	65	1.00	49
1.42	72	1.25	66
1.53	77	1.50	77
1.75	84	1.75	83
2.00	88	2.00	88
2.25	91	2.25	90
2.50	94		
2.75	94		
k_{obs} = 1.43 ± 0.04 h^{-1}. R^2 = 0.997		k_{obs} = 1.37 ± 0.06 h^{-1}. R^2 = 0.990	
M_n = 56 470 g mol^{-1}		M_n = 58 090 g mol^{-1}	
M_w/M_n = 1.17		M_w/M_n = 1.14	

[a]Conditions: [*L*-LA]$_0$:[**2**]$_0$ = 400:1, [*L*-LA]$_0$ = 0.5 M, [**2**]$_0$ = 0.00125 M, 7.0 mL benzene at 70 °C. Aliquots were taken at given intervals. [b]Measured by ^{1}H NMR spectroscopic analyses.

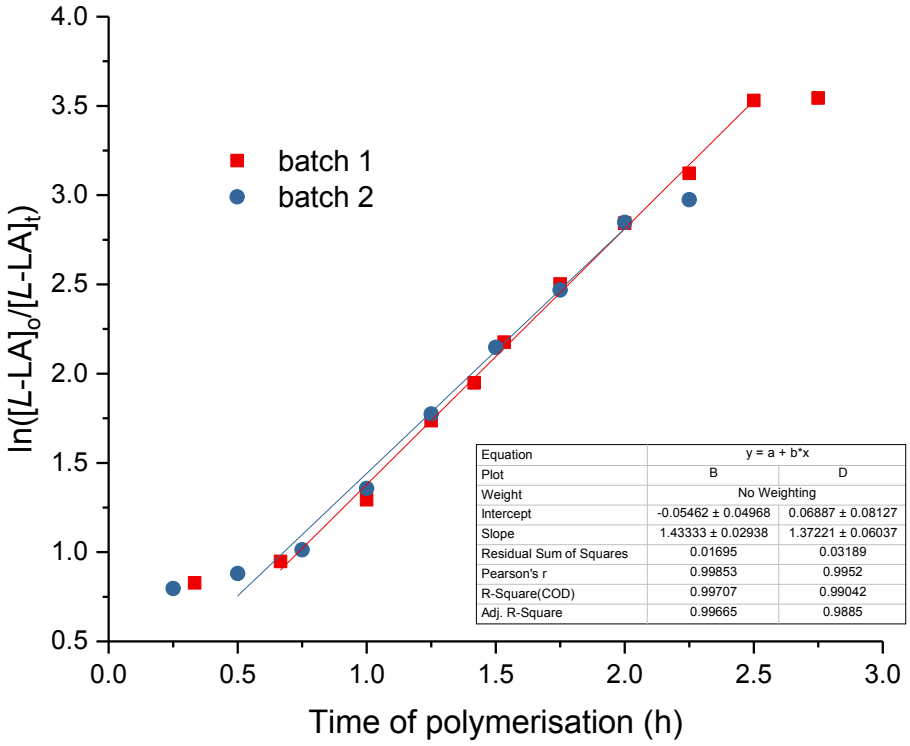

Fig. S41 plots of ln([*L*-LA]$_0$/[*L*-LA]$_t$) *vs.* time. Red squares: batch 1 (k_{obs} = 1.43 ± 0.04 h^{-1}. R^2 = 0.997), Blue circles: batch 2 (k_{obs} = 1.37 ± 0.06 h^{-1}. R^2 = 0.990). Conditions: [*L*-LA]$_0$:[**2**]$_0$ = 400:1, [*L*-LA]$_0$ = 0.5 M, [**2**]$_0$ = 0.00125 M, 7.0 mL benzene at 70 °C.

Table S9 ROP of *L*-LA using $^{Me}_2$SB(^{tBu}N,I*)Sc(O-2,6-^{i}Pr-C_6H_3)(THF) (**2**).[a]

$[L\text{-LA}]_0:[\mathbf{2}]_0$	Time (h)	Conv. (%)[b]	k_{obs} (h^{-1})[c]	R^{2c}	M_n (GPC)[d]	M_n (calcd)[e]	M_w/M_n
1000	3.75	90	0.70 ± 0.01	0.996	92 100	129 868	1.14
1000	4.00	90	0.66 ± 0.01	0.996	111 160	129 868	1.12
800	3.00	89	0.88 ± 0.03	0.991	82 290	102 777	1.13
800	3.00	90	0.82 ± 0.03	0.985	87 810	103 930	1.12
600	3.00	93	1.07 ± 0.04	0.988	68 220	80 586	1.14
600	3.00	91	1.00 ± 0.03	0.993	86 870	78 857	1.13
400	2.75	94	1.47 ± 0.05	0.995	56 470	54 359	1.17
400	2.25	90	1.37 ± 0.06	0.991	58 090	52 054	1.14

[a]Conditions: $[L\text{-LA}]_0:[\mathbf{2}]_0$ as stated, $[L\text{-LA}]_0$ = 0.5 M, 7.0 mL benzene at 70 °C. Polymerisations were quenched by THF. [b]Measured by ^{1}H NMR spectroscopic analyses. [c]First order rate constant with standard error and R^2 were determined by linear fit analysis. [d]Determined by GPC in chloroform at 30 °C against PS standards (M_n values are corrected by factor of 0.58).[3] [e]Calculated M_n for PLA terminated with –OH and –O-2,6-^{i}Pr-C_6H_3 groups = conv.(%) × $[L\text{-LA}]_0$:[initiator]$_0$ × 144.1 + 178.1

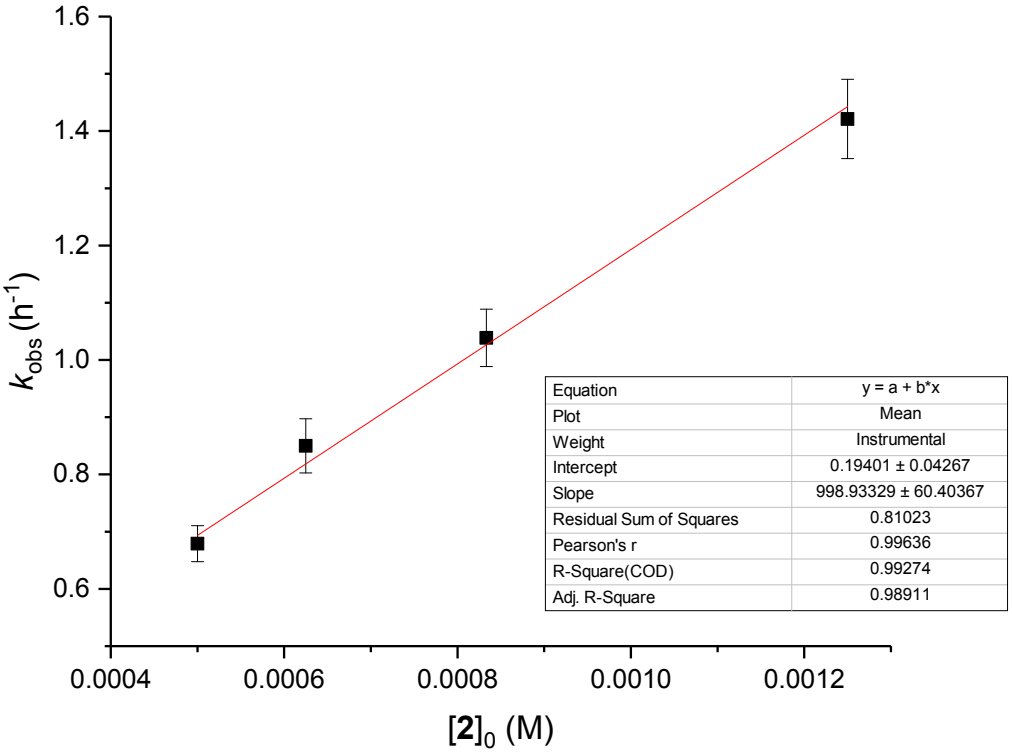

Fig. S42 Plot of k_{obs} *vs.* $[\mathbf{2}]_0$ for ROP of *L*-LA using **2**, k_p = 998 ± 60 $M^{-1}\,h^{-1}$, R^2 = 0.993.

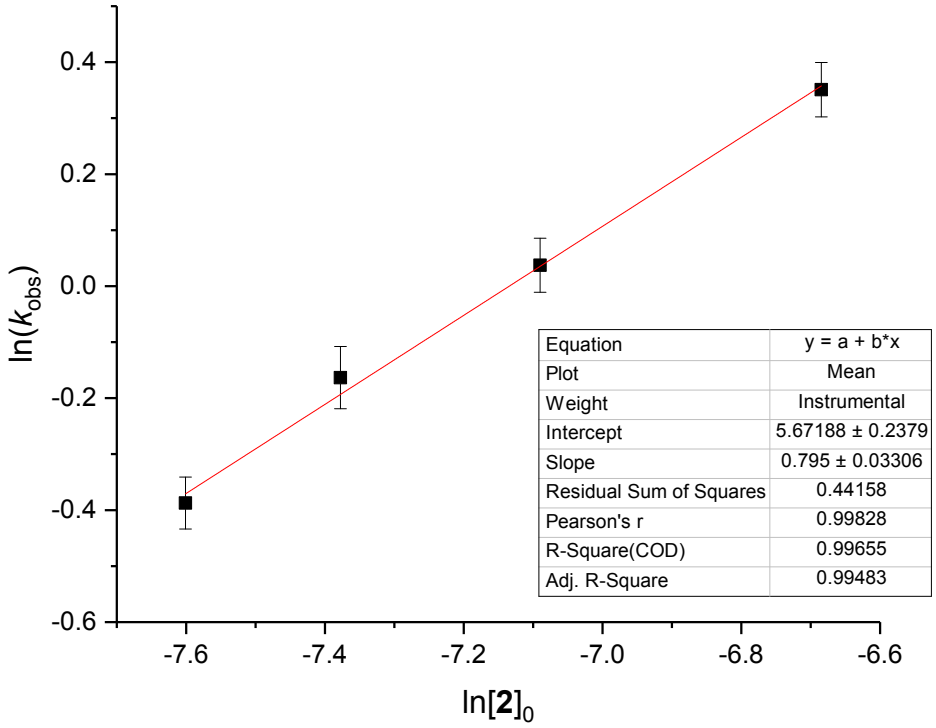

Fig. S43 Plot of -ln(k_{obs}) *vs.*-ln[**2**]$_0$ shows an order in concentration of **2** equal to 0.80 ± 0.03, R^2 = 0.997.

Table S10 ROP of *L*-LA using ^{Me2}SB(^{tBu}N,I*)Sc(O-2,6-^{i}Pr-C$_6$H$_3$)(THF) (**2**) at 60 °C.[a]

Time (h)	Conversion 1 (%)[b]	Time (h)	Conversion 2 (%)[b]
0.5	6		
1.0	9	1.0	11
1.5	16		
2.0	23	2.0	26
2.5	30		
3.0	38	3.0	46
3.5	46		
4.0	58	4.0	63
4.5	64		
5.0	70	5.0	77
5.5	77		
6.0	80	6.0	86
6.5	84		
		7.0	90
7.5	86		
8.0	89	8.0	92
k_{obs} = 0.32 ± 0.01 h^{-1}. R^2 = 0.986		k_{obs} = 0.38 ± 0.02 h^{-1}. R^2 = 0.987	
M_n = 114 870 g mol^{-1}		M_n = 124 050 g mol^{-1}	
M_w/M_n = 1.13		M_w/M_n = 1.12	

[a]Conditions: [*L*-LA]$_0$:[**2**]$_0$ = 1000:1, [*L*-LA]$_0$ = 0.5 M, [**2**]$_0$ = 0.0005 M, 7.0 mL benzene at 60 °C. Aliquots were taken at given intervals. [b]Measured by ^{1}H NMR spectroscopic analyses.

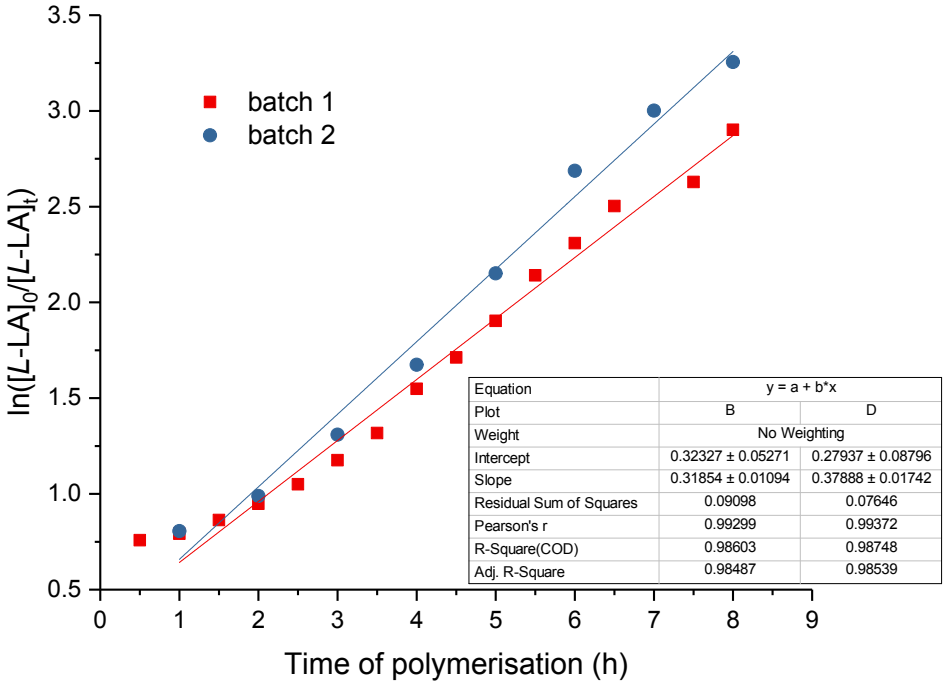

Fig. S44 plots of ln([*L*-LA]$_0$/[*L*-LA]$_t$) *vs.* time. Red squares: batch 1 (k_{obs} = 0.32 ± 0.01 h^{-1}. R^2 = 0.986), Blue circles: batch 2 (k_{obs} = 0.38 ± 0.02 h^{-1}. R^2 = 0.987). Conditions: [*L*-LA]$_0$:[**2**]$_0$ = 1000:1, [*L*-LA]$_0$ = 0.5 M, [**2**]$_0$ = 0.0005 M, 7.0 mL benzene at 60 °C.

Table S11 ROP of *L*-LA using ^{Me2}SB(^{tBu}N,I*)Sc(O-2,6-^{i}Pr-C_6H_3)(THF) (**2**) at 80 °C.[a]

Time (h)	Conversion 1 (%)[b]	Time (h)	Conversion 2 (%)[b]
0.25	7	0.25	7
0.50	17	0.50	22
0.75	31	0.75	41
1.00	46	1.00	58
1.25	59	1.25	73
1.50	70	1.50	81
1.75	77	1.75	85
2.00	83	2.00	89
2.25	86		
2.50	91		
k_{obs} = 1.06 ± 0.04 h^{-1}. R^2 = 0.990		k_{obs} = 1.26 ± 0.04 h^{-1}. R^2 = 0.994	
M_n = 108 920 g mol^{-1}		M_n = 98 560 g mol^{-1}	
M_w/M_n = 1.12		M_w/M_n = 1.10	

[a]Conditions: [*L*-LA]$_0$:[**2**]$_0$ = 1000:1, [*L*-LA]$_0$ = 0.5 M, [**2**]$_0$ = 0.0005 M, 7.0 mL benzene at 80 °C. Aliquots were taken at given intervals. [b]Measured by ^{1}H NMR spectroscopic analyses.

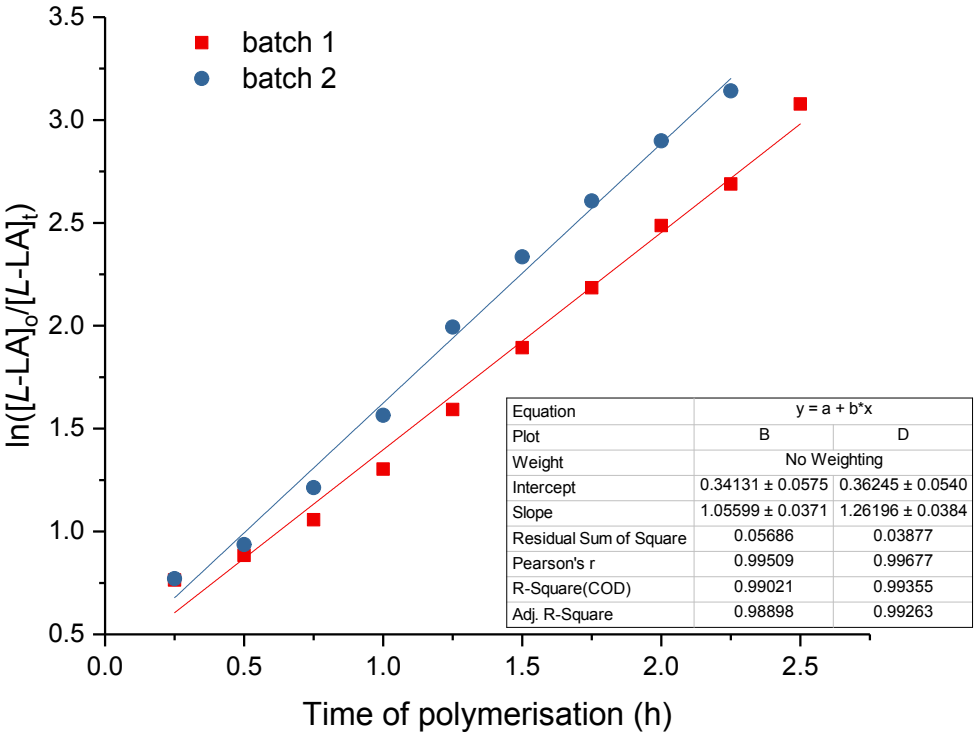

Fig. S45 plots of ln([*L*-LA]$_0$/[*L*-LA]$_t$) *vs.* time. Red squares: batch 1 (k_{obs} = 1.06 ± 0.04 h^{-1}. R^2 = 0.990), Blue circles: batch 2 (k_{obs} = 1.26 ± 0.04 h^{-1}. R^2 = 0.994). Conditions: [*L*-LA]$_0$:[**2**]$_0$ = 1000:1, [*L*-LA]$_0$ = 0.5 M, [**2**]$_0$ = 0.0005 M, 7.0 mL benzene at 80 °C.

Table S12 ROP of *L*-LA with $^{Me}_2$SB(^{tBu}N,I*)Sc(O-2,6-^{i}Pr-C_6H_3)(THF) (**2**) at various temperatures.[a]

T (°C)	Time (h)	Conv. (%)[b]	k_{obs} (h^{-1})[c]	R^{2}[c]	M_n (GPC)[d]	M_n (calcd)[e]	M_w/M_n
80	2.50	91	1.06 ± 0.04	0.990	108 920	131 309	1.12
80	2.00	89	1.26 ± 0.04	0.994	98 560	128 427	1.10
70	3.75	90	0.70 ± 0.01	0.996	92 100	129 868	1.14
70	4.00	90	0.66 ± 0.01	0.996	111 160	129 868	1.12
60	8.0	89	0.32 ± 0.01	0.986	114 870	128 427	1.13
60	8.0	92	0.38 ± 0.02	0.987	124 050	132 750	1.12

[a]Conditions: [*L*-LA]$_0$:[**2**]$_0$ = 1000, [*L*-LA]$_0$ = 0.5 M, 7.0 mL benzene at 80, 70 or 60 °C. All polymerisations were performed in duplicate. Polymerisations were quenched by THF. [b]Measured by ^{1}H NMR spectroscopic analyses. [c]First order rate constant with standard error and R^2 were determined by linear fit analysis. [d]Determined by GPC in chloroform at 30 °C against PS standards (M_n values are corrected by factor of 0.58).[3] [e]Calculated M_n for PLA terminated with –OH and –O-2,6-^{i}Pr-C_6H_3 groups = conv.(%) × [*L*-LA]$_0$:[initiator]$_0$ × 144.1 + 178.1.

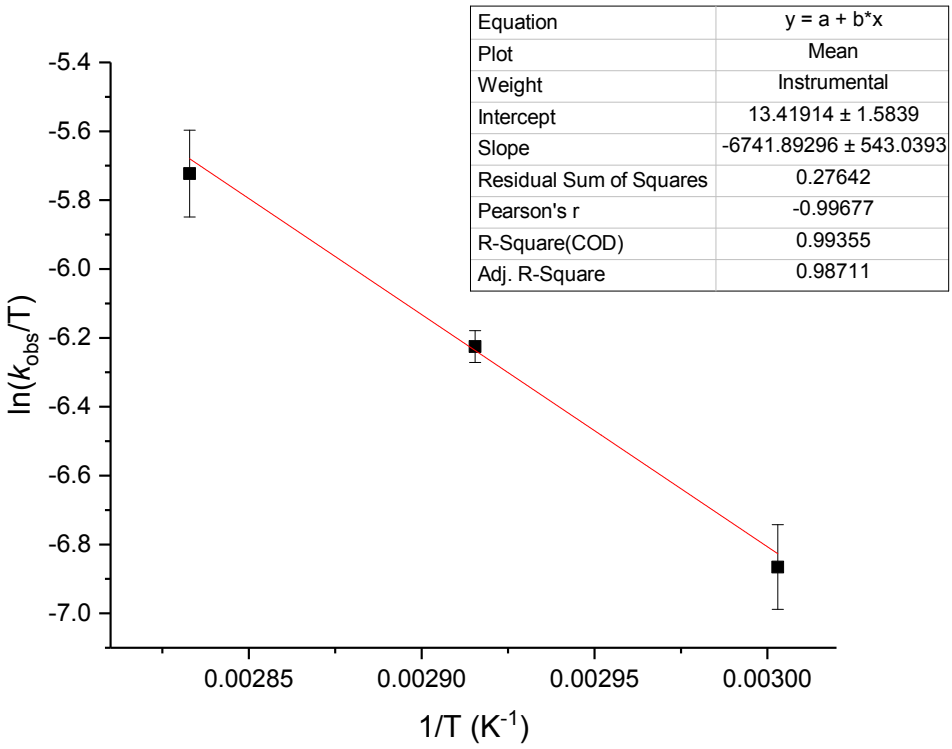

Fig. S46 Eyring plot of –ln(k_{obs}/T) *vs.* 1/T. Slope = -6741 ± 543, Intercept = 13 ± 1 with R^2 = 0.994. $\Delta H^{‡}$ = 56 ± 5 kJ mol^{-1}, $\Delta S^{‡}$ = -86 ± 13 J mol^{-1} K^{-1} for ROP of *L*-LA with $^{Me}_2$SB(^{tBu}N,I*)Sc(O-2,6-^{i}Pr-C_6H_3)(THF) (**2**).

Table S13 ROP of *rac*-LA with ^{Me2}SB(^{tBu}N,I*)Sc(O-2,6-^{i}Pr-C_6H_3)(THF) (**2**).[a]

Time (h)	Conversion 1 (%)[b]	Time (h)	Conversion 2 (%)[b]
0.3	13	0.3	14
0.5	45	0.5	48
0.8	73	0.8	76
1.0	86	1.0	88
		1.3	92
		1.5	94
k_{obs} = 2.46 ± 0.15 h^{-1}. R^2 = 0.992		k_{obs} = 2.46 ± 0.14 h^{-1}. R^2 = 0.990	
M_n = 82 380 g mol^{-1}		M_n = 92 640 g mol^{-1}	
M_w/M_n = 1.10		M_w/M_n = 1.10	
P_r (integration) = 0.71 ± 0.08		P_r (integration) = 0.65 ± 0.03	
P_r (deconvolution) = 0.71 ± 0.02		P_r (deconvolution) = 0.68 ± 0.01	

[a]Conditions: [*rac*-LA]$_0$:[**2**]$_0$ = 1000:1, [*rac*-LA]$_0$ = 0.5 M, [**2**]$_0$ = 0.0005 M, 7.0 mL benzene at 70 °C. Aliquots were taken at given intervals. [b]Measured by ^{1}H NMR spectroscopic analyses.

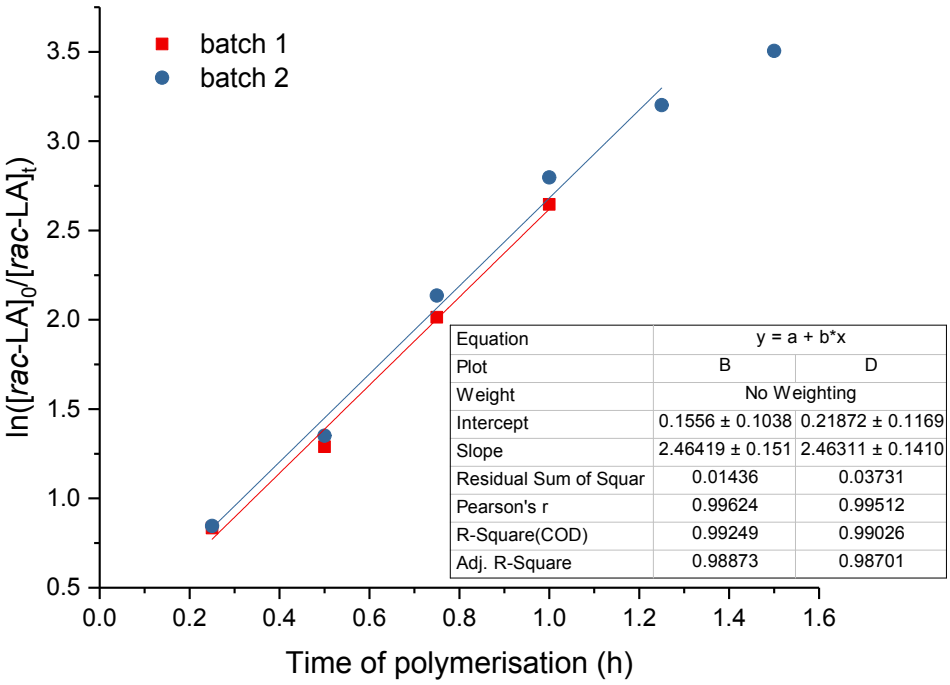

Fig. S47 plots of ln([*rac*-LA]$_0$/[*rac*-LA]$_t$) *vs.* time. Red squares: batch 1 (k_{obs} = 2.46 ± 0.15 h^{-1}. R^2 = 0.992), Blue circles: batch 2 (k_{obs} = 2.46 ± 0.14 h^{-1}. R^2 = 0.990). Conditions: [*rac*-LA]$_0$:[**2**]$_0$ = 1000:1, [*rac*-LA]$_0$ = 0.5 M, [**2**]$_0$ = 0.0005 M, 7.0 mL benzene at 70 °C.

Table S14 ROP of *L*-LA with ^{Me2}SB(^{tBu}N,I*)Sc(O-2,4-^{t}Bu-C_6H_3)(THF) (**3**) at 70 °C.[a]

Time (h)	Conversion 1 (%)[b]	Time (h)	Conversion 2 (%)[b]
0.13	8	0.13	8
0.18	27	0.18	25
0.23	60	0.23	59
0.28	78	0.28	76
0.33	85	0.33	86
0.38	90	0.38	89
0.43	92	0.43	92
k_{obs} = 8.81 ± 0.49 h^{-1}. R^2 = 0.985		k_{obs} = 8.67 ± 0.52 h^{-1}. R^2 = 0.982	

[a]Conditions: [*L*-LA]$_0$:[**3**]$_0$ = 1000:1, [*L*-LA]$_0$ = 0.5 M, [**3**]$_0$ = 0.0005 M, 7.0 mL benzene at 70 °C. Aliquots were taken at given intervals. [b]Measured by ^{1}H NMR spectroscopic analyses.

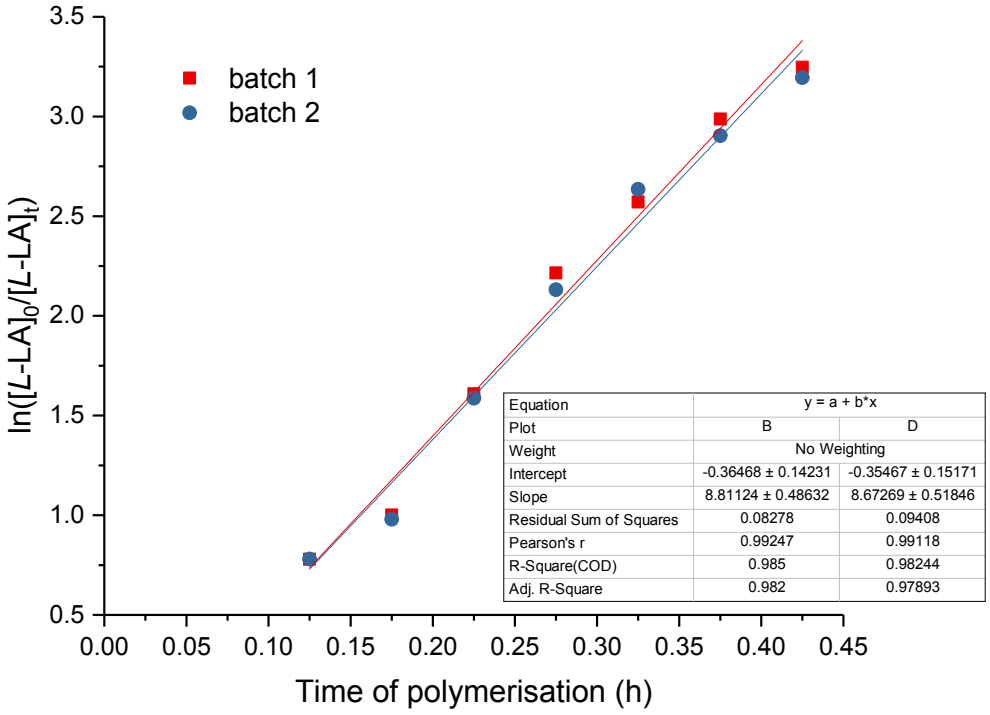

Figure S48 plots of ln([*L*-LA]$_0$/[*L*-LA]$_t$) *vs.* time. Red squares: batch 1 (k_{obs} = 8.81 ± 0.49 h^{-1}. R^2 = 0.985), Blue circles: batch 2 (k_{obs} = 8.67 ± 0.52 h^{-1}. R^2 = 0.982). Conditions: [*L*-LA]$_0$:[**3**]$_0$ = 1000:1, [*L*-LA]$_0$ = 0.5 M, [**3**]$_0$ = 0.0005 M, 7.0 mL benzene at 70 °C.

Table S15 ROP of *rac*-LA with ^{Me2}SB(^{tBu}N,I*)Sc(O-2,4-^{t}Bu-C_6H_3)(THF) (**3**) at 70 °C.[a]

Time (h)	Conversion 1 (%)[b]	Time (h)	Conversion 2 (%)[b]
0.13	8	0.13	9
0.20	26	0.20	27
0.25	51	0.25	58
0.30	73	0.30	78
0.35	82	0.35	86
0.40	88	0.40	90
0.45	91	0.45	92
0.50	92	0.50	94
0.58	94		
k_{obs} = 7.43 ± 0.46 h^{-1}. R^2 = 0.978		k_{obs} = 7.90 ± 0.52 h^{-1}. R^2 = 0.974	
P_r (integration) = 0.66 ± 0.07		P_r (integration) = 0.67 ± 0.05	
P_r (deconvolution) = 0.64 ± 0.04		P_r (deconvolution) = 0.65 ± 0.05	

[a]Conditions: [*rac*-LA]$_0$:[**3**]$_0$ = 1000:1, [*rac*-LA]$_0$ = 0.5 M, [**3**]$_0$ = 0.0005 M, 7.0 mL benzene at 70 °C. Aliquots were taken at given intervals. [b]Measured by ^{1}H NMR spectroscopic analyses.

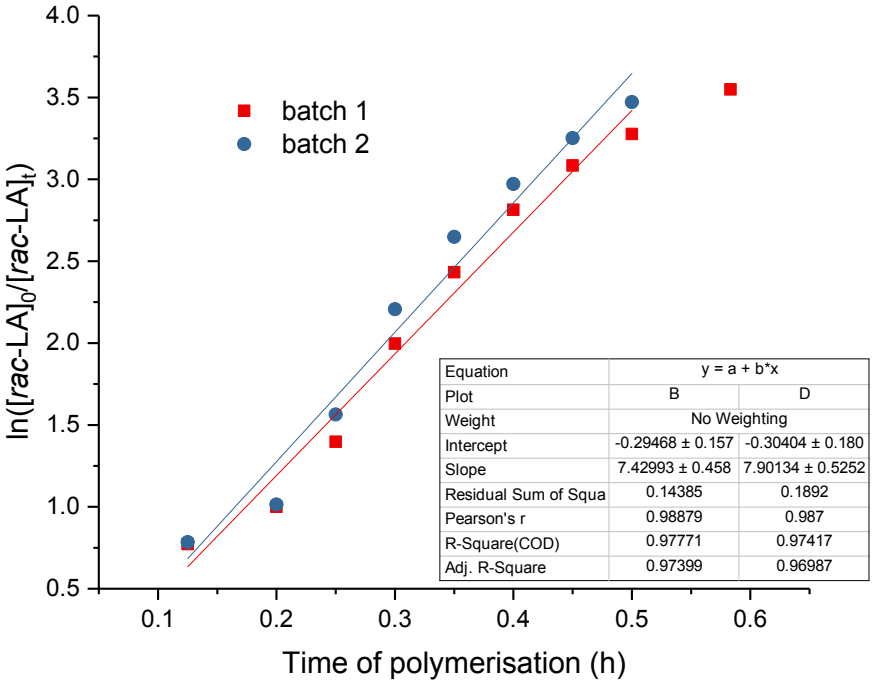

Figure S49 plots of ln([*rac*-LA]$_0$/[*rac*-LA]$_t$) *vs.* time. Red squares: batch 1 (k_{obs} = 7.43 ± 0.46 h^{-1}. R^2 = 0.989), Blue circles: batch 2 (k_{obs} = 7.90 ± 0.52 h^{-1}. R^2 = 0.987). Conditions: [*L*-LA]$_0$:[**3**]$_0$ = 1000:1, [*rac*-LA]$_0$ = 0.5 M, [**3**]$_0$ = 0.0005 M, 7.0 mL benzene at 70 °C.

Table S16 ROP of *L*-LA with ^{Me2}SB(^{tBu}N,I*)Sc(O-2,4-^{t}Bu-C_6H_3)(THF) (**3**) at 60 °C.[a]

Time (h)	Conversion 1 (%)[b]	Time (h)	Conversion 2 (%)[b]
0.17	7	0.17	7
0.25	15	0.25	15
0.29	29	0.29	28
0.33	47	0.33	44
0.38	61	0.38	59
0.42	71	0.42	69
0.46	80	0.46	76
0.50	85	0.50	83
		0.58	88
		0.67	91
k_{obs} = 7.09 ± 0.22 h^{-1}. R^2 = 0.995		k_{obs} = 5.72 ± 0.26 h^{-1}. R^2 = 0.985	

[a]Conditions: [*L*-LA]$_0$:[**3**]$_0$ = 1000:1, [*L*-LA]$_0$ = 0.5 M, [**3**]$_0$ = 0.0005 M, 7.0 mL benzene at 60 °C. Aliquots were taken at given intervals. [b]Measured by ^{1}H NMR spectroscopic analyses.

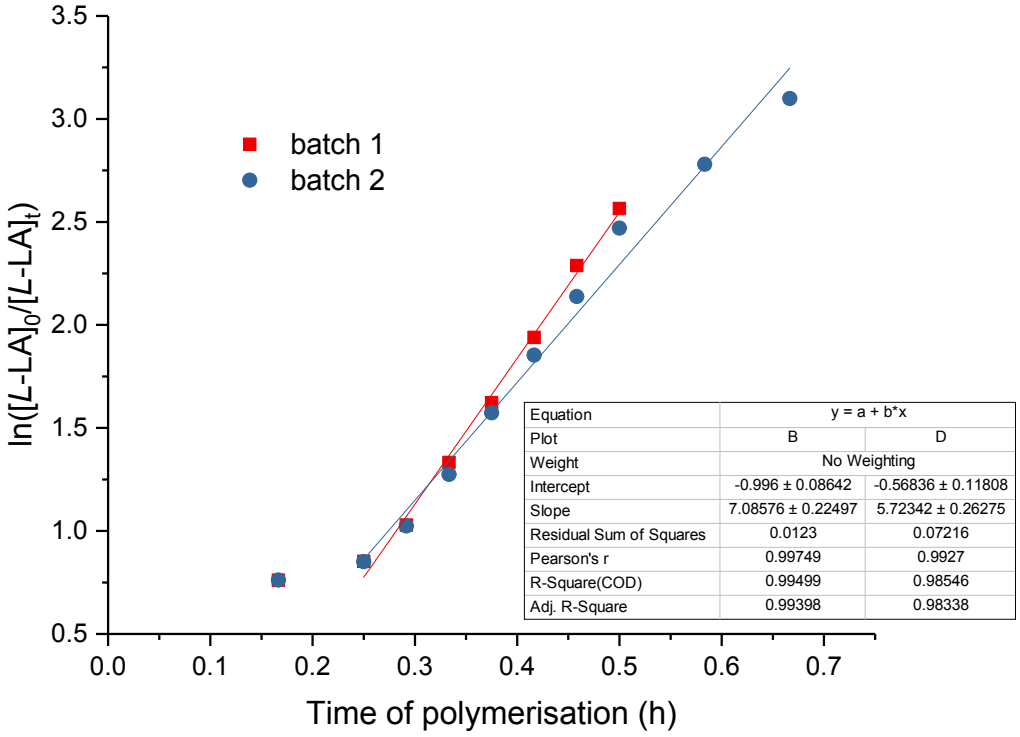

Figure S50 plots of ln([*L*-LA]$_0$/[*L*-LA]$_t$) *vs.* time. Red squares: batch 1 (k_{obs} = 7.09 ± 0.22 h^{-1}. R^2 = 0.995), Blue circles: batch 2 (k_{obs} = 5.72 ± 0.26 h^{-1}. R^2 = 0.985). Conditions: [*L*-LA]$_0$:[**3**]$_0$ = 1000:1, [*rac*-LA]$_0$ = 0.5 M, [**3**]$_0$ = 0.0005 M, 7.0 mL benzene at 60 °C.

Table S17 ROP of *L*-LA with $^{Me}_2$SB($^{t\text{Bu}}$N,I*)Sc(O-2,4-^{t}Bu-C_6H_3)(THF) (**3**) at 50 °C.[a]

Time (h)	Conversion 1 (%)[b]	Time (h)	Conversion 2 (%)[b]
0.13	4	0.13	3
0.25	6	0.25	6
0.38	9	0.38	10
0.50	20	0.50	22
0.58	36	0.58	39
0.67	60	0.67	58
0.75	73	0.75	71
0.83	81	0.83	80
0.92	86	0.92	85
1.00	89	1.00	88
k_{obs} = 4.17 ± 0.17 h^{-1}. R^2 = 0.992		k_{obs} = 3.91 ± 0.15 h^{-1}. R^2 = 0.993	
M_n = 122 520 g mol^{-1}		M_n = 126 400 g mol^{-1}	
M_w/M_n = 1.14		M_w/M_n = 1.09	

[a]Conditions: $[L\text{-LA}]_0$:[**3**]$_0$ = 1000:1, $[L\text{-LA}]_0$ = 0.5 M, [**3**]$_0$ = 0.0005 M, 7.0 mL benzene at 50 °C. Aliquots were taken at given intervals. [b]Measured by ^{1}H NMR spectroscopic analyses.

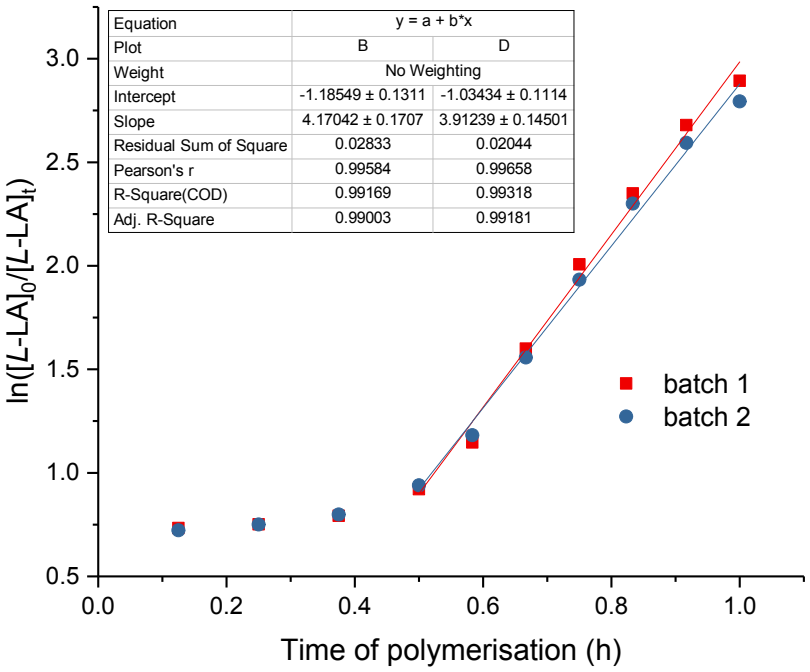

Fig. S51 plots of ln($[L\text{-LA}]_0/[L\text{-LA}]_t$) *vs.* time. Red squares: batch 1 (k_{obs} = 4.17 ± 0.17 h^{-1}. R^2 = 0.992), Blue circles: batch 2 (k_{obs} = 3.91 ± 0.15 h^{-1}. R^2 = 0.993). Conditions: $[L\text{-LA}]_0$:[**3**]$_0$ = 1000:1, $[L\text{-LA}]_0$ = 0.5 M, [**3**]$_0$ = 0.0005 M, 7.0 mL benzene at 50 °C.

Table S18 ROP of *rac*-LA with ^{Me_2}SB(^{tBu}N,I*)Sc(O-2,4-^{t}Bu-C_6H_3)(THF) (**3**) at 50 °C.[a]

Time (h)	Conversion 1 (%)[b]	Time (h)	Conversion 2 (%)[b]
0.50	11	0.50	11
0.58	15	0.58	15
0.67	23	0.67	21
0.75	34	0.75	30
0.83	53	0.83	46
0.92	66	0.92	62
1.00	76	1.00	73
1.08	83	1.08	81
1.17	87	1.17	86
1.25	90	1.25	90
		1.33	91
		1.42	93
		1.50	94
k_{obs} = 3.71 ± 0.10 h^{-1}. R^2 = 0.996		k_{obs} = 3.70 ± 0.15 h^{-1}. R^2 = 0.991	
M_n = 98 360 g mol^{-1}		M_n = 129 940 g mol^{-1}	
M_w/M_n = 1.18		M_w/M_n = 1.10	
P_r (integration) = 0.67 ± 0.05		P_r (integration) = 0.66 ± 0.04	
P_r (deconvolution) = 0.72 ± 0.12		P_r (deconvolution) = 0.70 ± 0.03	

[a]Conditions: [*rac*-LA]$_0$:[**3**]$_0$ = 1000:1, [*rac*-LA]$_0$ = 0.5 M, [**3**]$_0$ = 0.0005 M, 7.0 mL benzene at 50 °C. Aliquots were taken at given intervals. [b]Measured by ^{1}H NMR spectroscopic analyses.

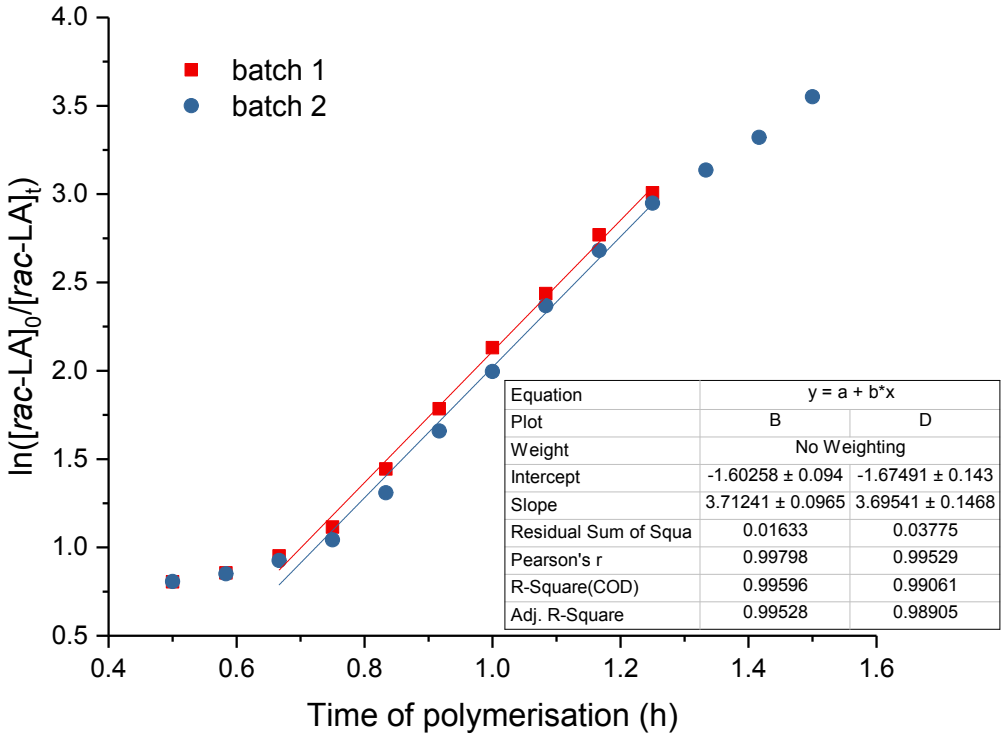

Fig. S52 plots of ln([*rac*-LA]$_0$/[*rac*-LA]$_t$) *vs.* time. Red squares: batch 1 (k_{obs} = 3.71 ± 0.10 h^{-1}. R^2 = 0.996), Blue circles: batch 2 (k_{obs} = 3.70 ± 0.15 h^{-1}. R^2 = 0.991). Conditions: [*rac*-LA]$_0$:[**3**]$_0$ = 1000:1, [*rac*-LA]$_0$ = 0.5 M, [**3**]$_0$ = 0.0005 M, 7.0 mL benzene at 50 °C.

Table S19 ROP of *L*-LA with ^{Me2}SB(^{tBu}N,I*)Sc(O-2,4-^{t}Bu-C$_6$H$_3$)(THF) (**3**) at various temperatures.[a]

T (°C)	Time (h)	Conv. (%)[b]	k_{obs} (h^{-1})[c]	R^{2c}
70	0.43	92	8.81 ± 0.49	0.992
70	0.43	92	8.67 ± 0.52	0.991
60	0.50	85	7.09 ± 0.22	0.995
60	0.67	91	5.72 ± 0.26	0.985
50	1.00	89	4.17 ± 0.17	0.992
50	1.00	88	3.91 ± 0.15	0.993

[a]Conditions: [*L*-LA]$_0$:[**3**]$_0$ = 1000, [*L*-LA]$_0$ = 0.5 M, 7.0 mL benzene at 70, 60 or 50 °C. All polymerisations were performed in duplicate. Polymerisations were quenched by THF. [b]Measured by ^{1}H NMR spectroscopic analyses. [c]First order rate constant with standard error and R^2 were determined by linear fit analysis.

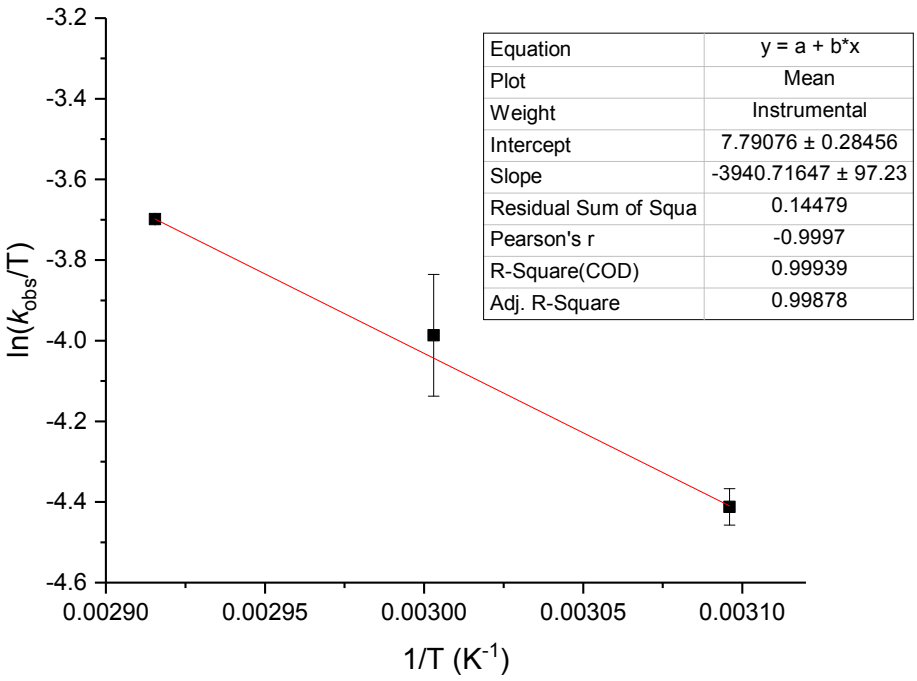

Figure S53 Eyring plot of –ln(k_{obs}/T) *vs.* 1/T. Slope = -3940 ± 97, Intercept = 7.8 ± 0.3 with R^2 = 0.999. $\Delta H^{\ddagger}$ = 33 ± 1 kJ mol^{-1}, $\Delta S^{\ddagger}$ = -133 ± 2 J mol^{-1} K^{-1} for ROP of *L*-LA with ^{Me2}SB(^{tBu}N,I*)Sc(O-2,4-^{t}Bu-C$_6$H$_3$)(THF) (**3**).

Table S20 ROP of *L*-LA with ^{Me2}SB(^{tBu}N,I*)Sc(BH$_4$)(THF) (**4**).[a]

Time (h)	Conversion 1 (%)[b]	Time (h)	Conversion 2 (%)[b]
0.12	23	0.12	24
0.17	37	0.17	39
0.21	48	0.21	48
0.25	57	0.25	55
0.29	63	0.29	60
0.33	69	0.33	65
0.42	75	0.42	71
0.50	75	0.50	74
0.58	82	0.58	77
0.67	83	0.67	81
k_{obs} = 17.29 ± 0.89 M^{-1}h^{-1}. R^2 = 0.979		k_{obs} = 13.88 ± 0.30 M^{-1}h^{-1}. R^2 = 0.996	
M_n = 81 780 g mol^{-1}		M_n = 65 930 g mol^{-1}	
M_w/M_n = 1.24		M_w/M_n = 1.25	

[a]Conditions: [*L*-LA]$_0$:[**4**]$_0$ = 1000:1, [*L*-LA]$_0$ = 0.5 M, [**4**]$_0$ = 0.0005 M, 7.0 mL benzene at 50 °C. Aliquots were taken at given intervals. [b]Measured by ^{1}H NMR spectroscopic analyses.

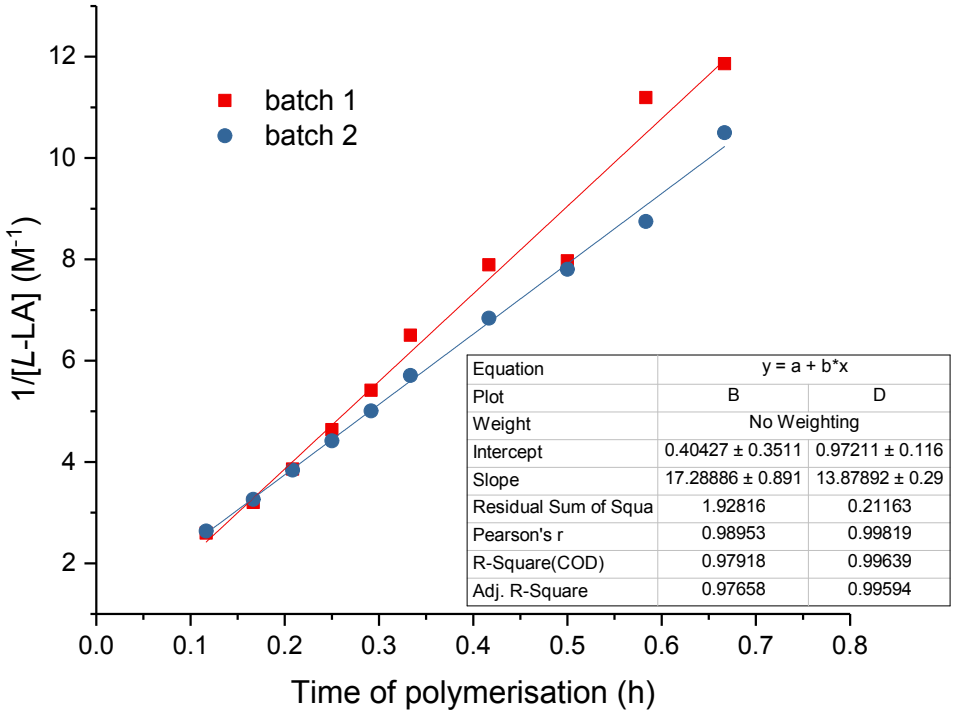

Fig. S54 plots of ln([*L*-LA]$_0$/[*L*-LA]$_t$) *vs.* time. Red squares: batch 1 (k_{obs} = 17.29 ± 0.89 M^{-1}h^{-1}. R^2 = 0.979), Blue circles: batch 2 (k_{obs} = 13.88 ± 0.30 M^{-1}h^{-1}. R^2 = 0.996). Conditions: [*L*-LA]$_0$:[**4**]$_0$ = 1000:1, [*L*-LA]$_0$ = 0.5 M, [**4**]$_0$ = 0.0005 M, 7.0 mL benzene at 50 °C.

Table S21 ROP of *rac*-LA with ^{Me2}SB(^{tBu}N,I*)Sc(BH$_4$)(THF) (**4**).[a]

Time (h)	Conversion 1 (%)[b]	Time (h)	Conversion 2 (%)[b]
0.17	24	0.17	27
0.21	41	0.21	43
0.25	57	0.25	56
0.29	67	0.29	65
0.33	75	0.33	72
0.42	82	0.42	81
0.50	86	0.50	86
0.58	89	0.58	88
0.67	91	0.67	90
k_{obs} = 40.70 ± 1.48 M^{-1}h^{-1}. R^2 = 0.991		k_{obs} = 36.64 ± 1.14 h^{-1}. R^2 = 0.993	
M_n = 60 730 g mol^{-1}		M_n = 72 830 g mol^{-1}	
M_w/M_n = 1.26		M_w/M_n = 1.24	
P_r (integration) = 0.67		P_r (integration) = 0.63	
P_r (deconvolution) = 0.67		P_r (deconvolution) = 0.63	

[a]Conditions: [*rac*-LA]$_0$:[**4**]$_0$ = 1000:1, [*rac*-LA]$_0$ = 0.5 M, [**4**]$_0$ = 0.0005 M, 7.0 mL benzene at 50 °C. Aliquots were taken at given intervals. [b]Measured by ^{1}H NMR spectroscopic analyses.

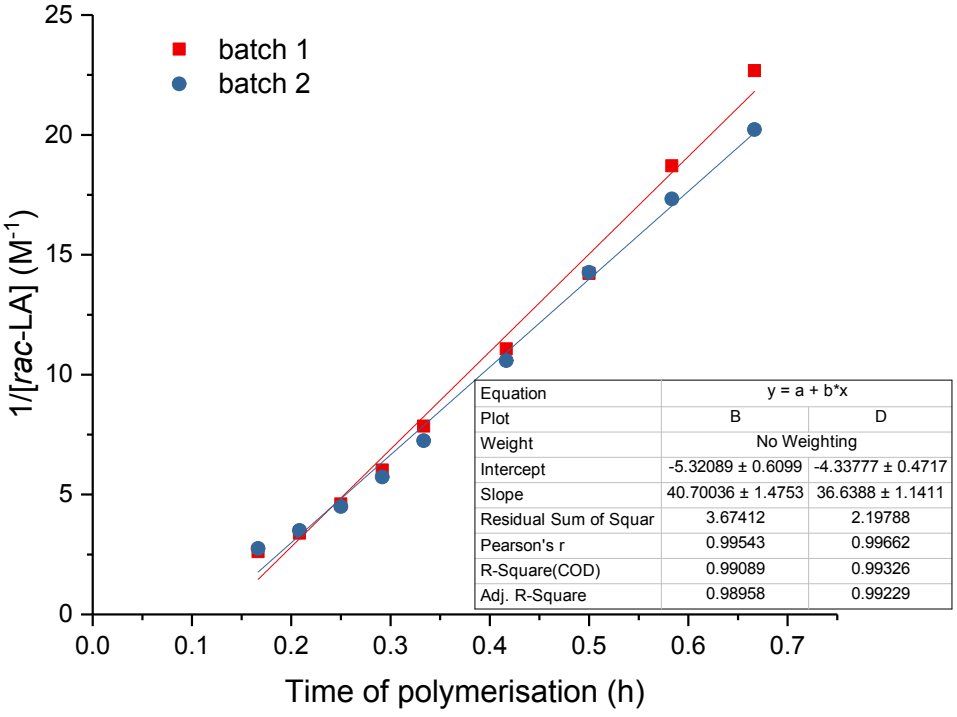

Fig. S55 plots of ln([*rac*-LA]$_0$/[*rac*-LA]$_t$) *vs.* time. Red squares: batch 1 (k_{obs} = 40.70 ± 1.48 M^{-1}h^{-1}. R^2 = 0.991), Blue circles: batch 2 (k_{obs} = 36.64 ± 1.14 h^{-1}. R^2 = 0.993). Conditions: [*rac*-LA]$_0$:[**4**]$_0$ = 1000:1, [*rac*-LA]$_0$ = 0.5 M, [**4**]$_0$ = 0.0005 M, 7.0 mL benzene at 50 °C.

Additional GPC data

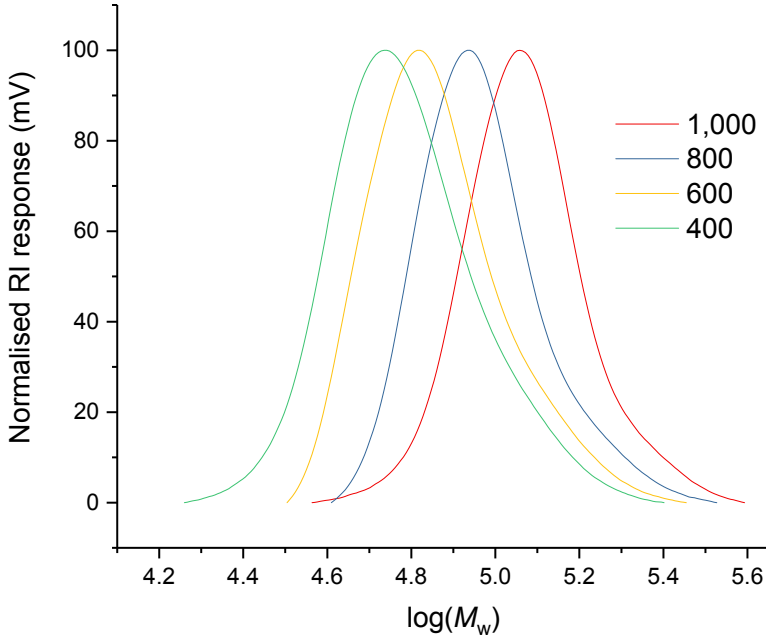

Fig. S56 Stacked GPC traces of PLAs synthesised from the ROP of *L*-LA using ^{Me2}SB(^{tBu}N,I*)Sc(O-2,6-^{i}Pr-C$_6$H$_3$)(THF) (**2**). Red: [*L*-LA]$_0$:[**2**]$_0$ = 1000, M_n = 111 160 g mol^{-1}, M_w/M_n = 1.12, Blue: [*L*-LA]$_0$:[**2**]$_0$ = 800, M_n = 87 810 g mol^{-1}, M_w/M_n = 1.12, Yellow: [*L*-LA]$_0$:[**2**]$_0$ = 600, M_n = 68 220 g mol^{-1}, M_w/M_n = 1.14, Green: [*L*-LA]$_0$:[**2**]$_0$ = 400, M_n = 56 470 g mol^{-1}, M_w/M_n = 1.17, Conditions: [*L*-LA]$_0$:[**2**]$_0$ as stated, [*L*-LA]$_0$ = 0.5 M, 7.0 mL benzene at 70 °C.

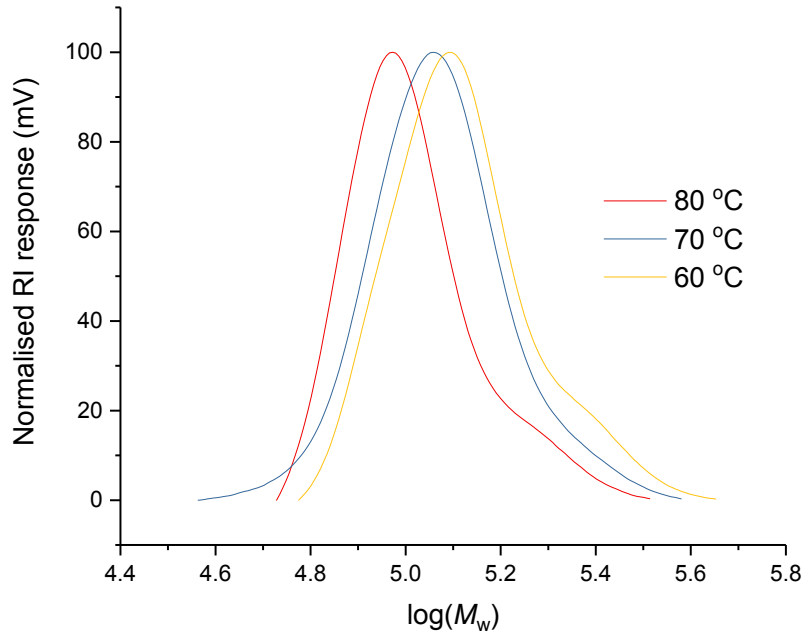

Fig. S57 Stacked GPC traces of PLAs synthesised from the ROP of *L*-LA using ^{Me2}SB(^{tBu}N,I*)Sc(O-2,6-^{i}Pr-C$_6$H$_3$)(THF) (**2**) at various temperatures. Red: *T* = 80 °C, M_n = 98 560 g mol^{-1}, M_w/M_n = 1.10, Blue: *T* = 70 °C, M_n = 111 160 g mol^{-1}, M_w/M_n = 1.12, Yellow: *T* = 60 °C, M_n = 124 050 g mol^{-1}, M_w/M_n = 1.12. Conditions: [*L*-LA]$_0$:[**2**]$_0$ = 1000, [*L*-LA]$_0$ = 0.5 M, 7.0 mL benzene at 60, 70 and 80 °C.

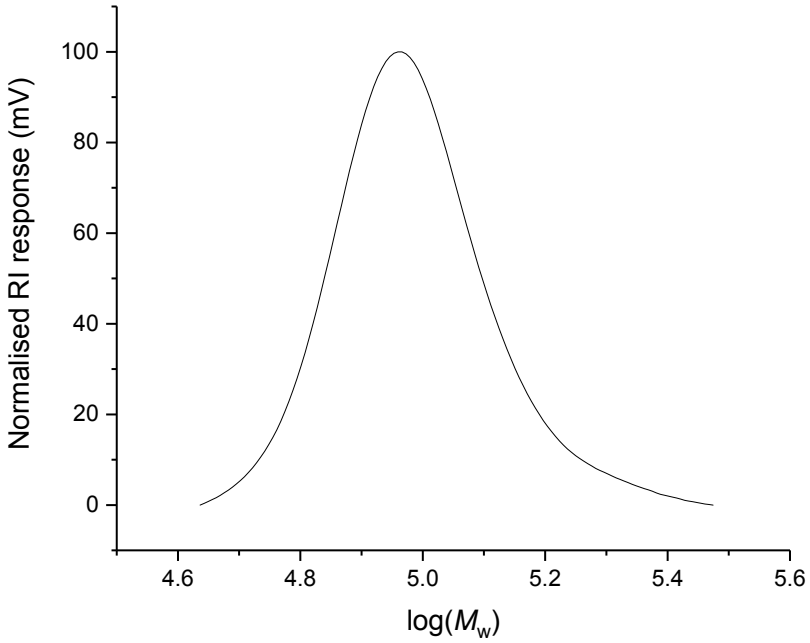

Fig. S58 GPC traces of PLA synthesised from the ROP of *rac*-LA using ^{Me2}SB(^{tBu}N,I*)Sc(O-2,6-^{i}Pr-C_6H_3)(THF) (**2**). M_n = 92 640 g mol^{-1}, M_w/M_n = 1.10. Conditions: [*rac*-LA]$_0$:[**2**]$_0$ = 1000, [*rac*-LA]$_0$ = 0.5 M, 7.0 mL benzene at 70 °C.

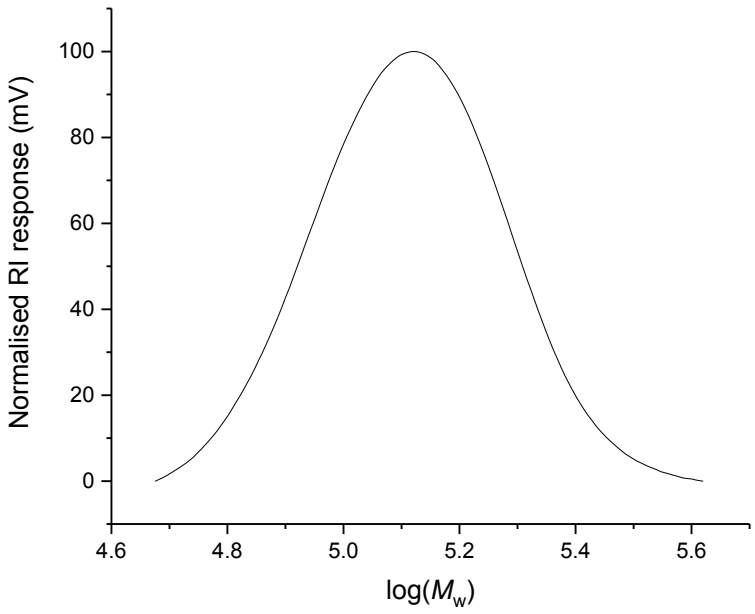

Fig. S59 GPC traces of PLA synthesised from the ROP of *L*-LA using ^{Me2}SB(^{tBu}N,I*)Sc(O-2,4-^{t}Bu-C_6H_3)(THF) (**2**). M_n = 126 400 g mol^{-1}, M_w/M_n = 1.10. Conditions: [*L*-LA]$_0$:[**2**]$_0$ = 1000, [*L*-LA]$_0$ = 0.5 M, 7.0 mL benzene at 50 °C.

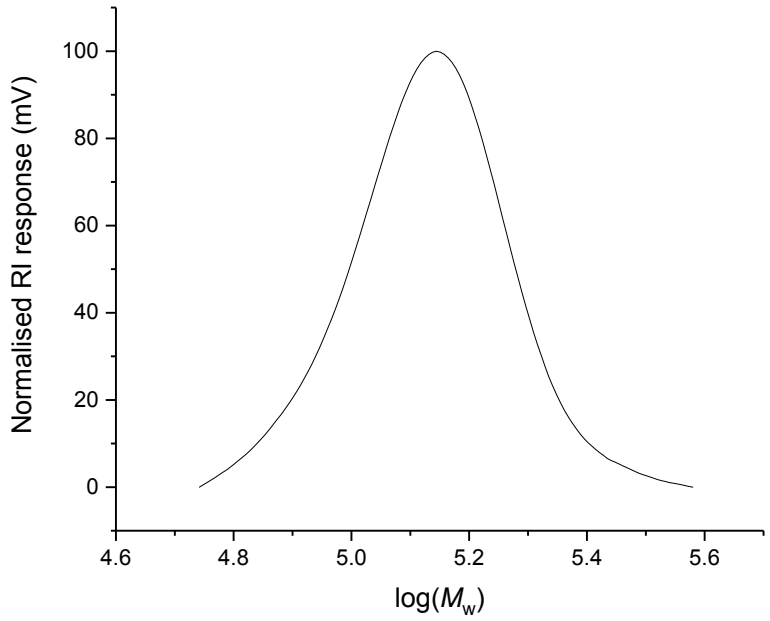

Fig. S60 GPC traces of PLA synthesised from the ROP of *rac*-LA using $^{Me}_2$SB(^{tBu}N,I*)Sc(O-2,4-^{t}Bu-C_6H_3)(THF) (**3**). M_n = 129 940 g mol^{-1}, M_w/M_n = 1.10. Conditions: [*rac*-LA]$_0$:[**3**]$_0$ = 1000, [*rac*-LA]$_0$ = 0.5 M, 7.0 mL benzene at 50 °C.

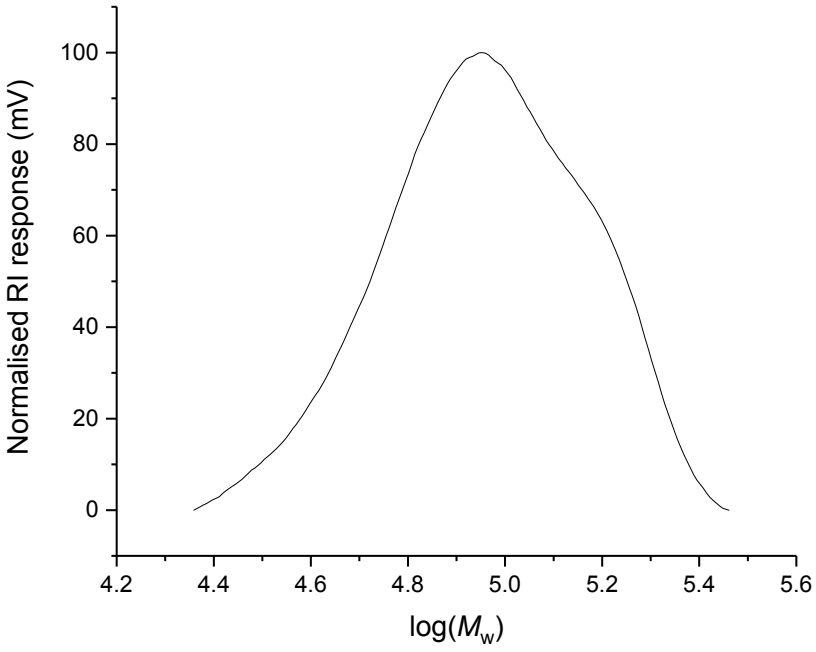

Fig. S61 GPC traces of PLA synthesised from the ROP of *L*-LA using $^{Me}_2$SB(^{tBu}N,I*)Sc(BH_4)(THF) (**4**). M_n = 65 930 g mol^{-1}, M_w/M_n = 1.25. Conditions: [*L*-LA]$_0$:[**4**]$_0$ = 1000, [*L*-LA]$_0$ = 0.5 M, 7.0 mL benzene at 50 °C.

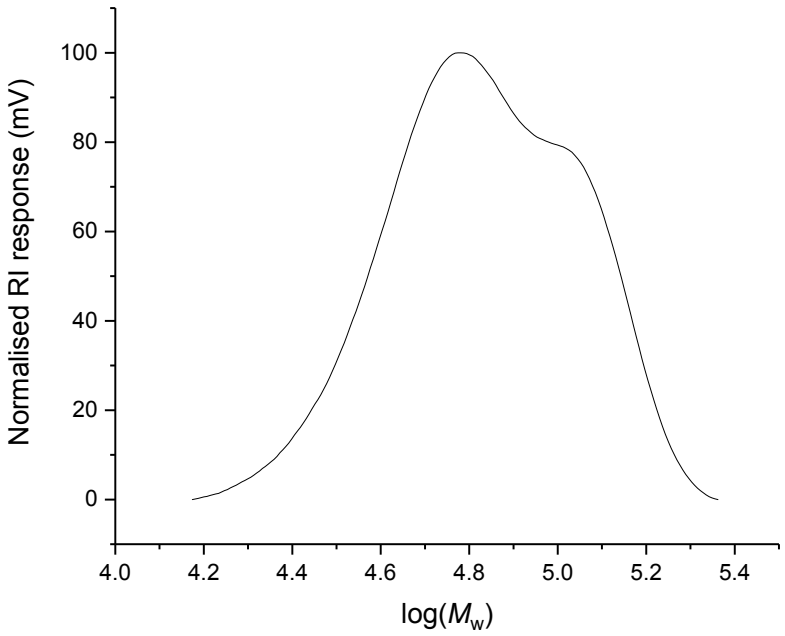

Fig. S62 GPC traces of PLA synthesised from the ROP of *rac*-LA using ^{Me2}SB(^{tBu}N,I*)Sc(BH_4)(THF) (**4**). M_n = 60 730 g mol^{-1}, M_w/M_n = 1.26. Conditions: [*rac*-LA]$_0$:[**4**]$_0$ = 1000, [*rac*-LA]$_0$ = 0.5 M, 7.0 mL benzene at 50 °C.

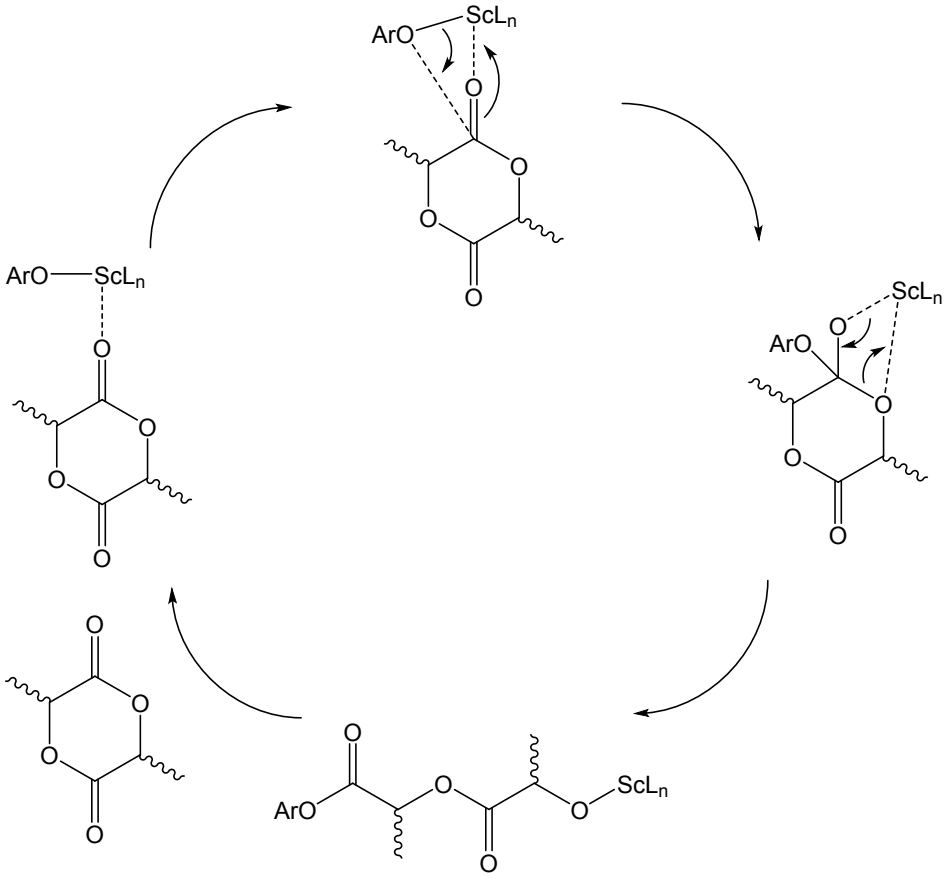

Fig. S63 Coordination-insertion mechanism for ring-opening polymerisation of lactide using ^{Me_2}SB(^{tBu}N,I*)Sc(O-2,6-^{i}Pr-C_6H_3)(THF) (**2**) or ^{Me_2}SB(^{tBu}N,I*)Sc(O-2,4-^{t}Bu-C_6H_3)(THF) (**3**). L_n = ^{Me_2}SB(^{tBu}N,I*).

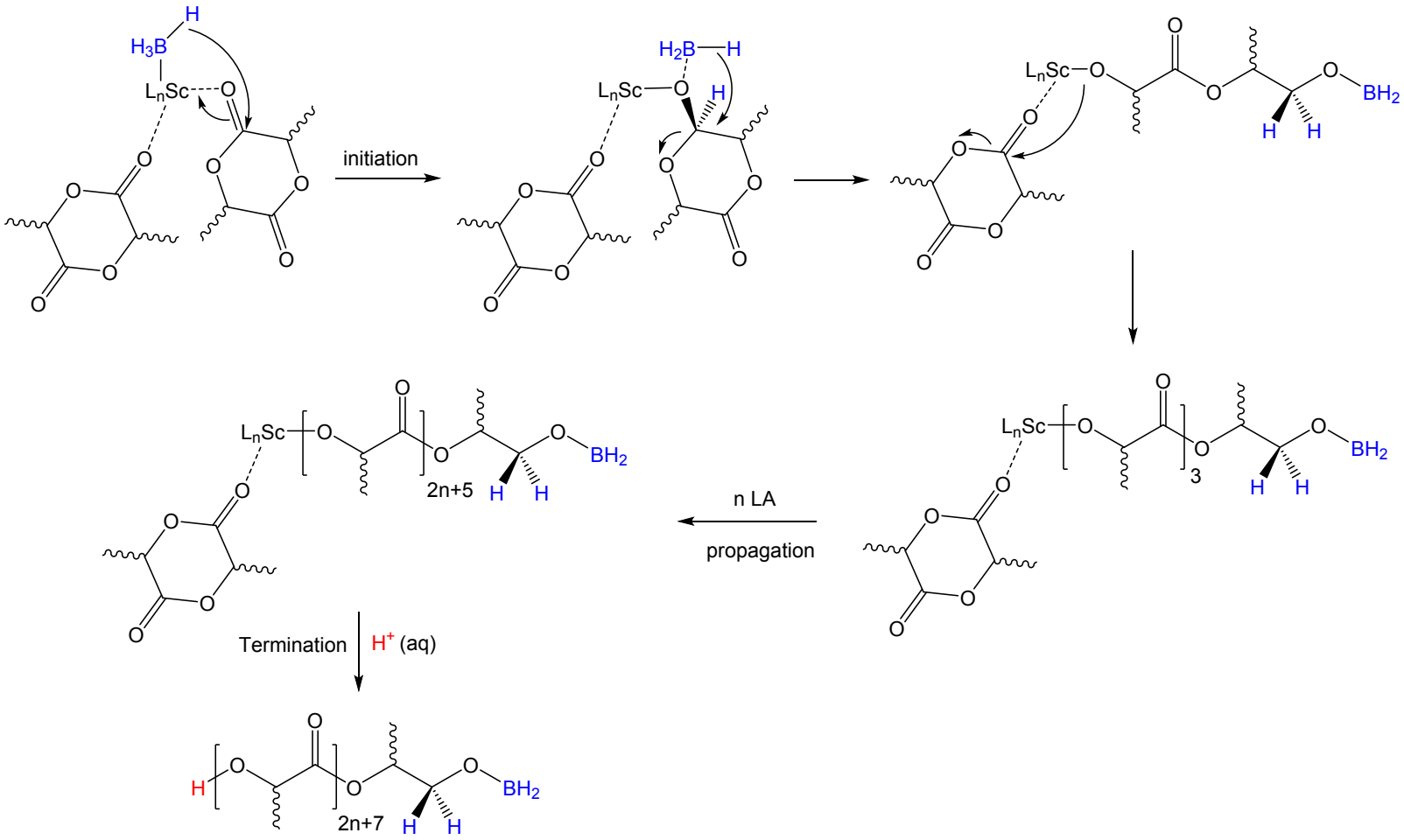

Fig. S64 Proposed mechanism for ring-opening polymerisation of lactide initiated by ^{Me_2}SB(^{tBu}N,I*)Sc(BH$_4$)(THF) (**4**). L$_n$ = ^{Me_2}SB(^{tBu}N,I*).

References

1. P. McKeown, M. G. Davidson, G. Kociok-Köhn and M. D. Jones, *Chem. Commun.*, 2016, **52**, 10431-10434.
2. J. Coudane, C. Ustariz-Peyret, G. Schwach and M. Vert, *J. Polym. Sci. A Polym. Chem.*, 1997, **35**, 1651-1658.
3. (a) A. Kowalski, A. Duda and S. Penczek, *Macromolecules*, 1998, **31**, 2114-2122; (b) M. Save, M. Schappacher and A. Soum, *Macromol. Chem. Phys.*, 2002, **203**, 889-899.
4. J. Cosier and A. M. Glazer, *J. Appl. Cryst.*, 1986, **19**, 105-107.
5. CrysAlisPRO, Oxford Diffraction /Agilent Technologies UK Ltd, Yarnton, England.
6. A. Altomare, G. Cascarano, C. Giacovazzo and A. Guagliardi, *J. Appl. Cryst.*, 1993, **26**, 343-350.
7. L. Palatinus and G. Chapuis, *J. Appl. Cryst.*, 2007, **40**, 786-790.
8. L. Farrugia, *J. Appl. Cryst.*, 1999, **32**, 837-838.
9. J.-C. Buffet, T. A. Q. Arnold, Z. R. Turner, P. Angpanitcharoen and D. O'Hare, *RSC Adv.*, 2015, **5**, 87456-87464.